COMPETITIVE GEOMETRIC EVOLUTION OF AMPHIPHILIC INTERFACES

SHIBIN DAI* AND KEITH PROMISLOW†

Abstract. We derive the curvature driven flow of closed-loop pore structures which arise a quasi-stationary states in the H^{-1} gradient flow of the Functionalized Cahn-Hilliard free energy which models amphiphilic mixtures. We extend this result to a sharp-interface reduction for the competitive evolution of disjoint collections of bilayer interfaces and closed-loop pores. In particular, for a mixture of spherical bilayers and circular, closed pores we explicitly identify two regimes: one in which spherical bilayers extinguish and the circular pores arrive at a common radius, and a complimentary regime in which spherical bilayers of differing radii stably coexist with common-radius, closed-loop, circular pores.

1. Introduction. Amphiphilic molecules, commonly used as surfactants, possess a hydrophilic and a hydrophobic moiety; when mixed with a suitable solvent the amphiphilic molecules form molecular-width bilayer interfaces and pore structures which interpenetrate the bulk regions of the solvent phase. The amphiphilic nature of the surfactant phase drives interfacial dynamics that are fundamentally different from those observed in mixtures of mutually non-wetting phases. Indeed, the surfactant phase seeks to maximize the interface between hydrophilic groups and solvent, subject to the constraint imposed by available surfactant volume.

In energy conversion materials, such as polymer electrolyte membranes, hydrophilic head groups are tethered to spatially extended hydrophobic polymers, forming an amphiphilic matrix which imbibes solvent, forming counter-ion conducting networks of solvent-filled pores with dominant length-scales ranging from 1-4 nanometers and solvent accessible surface areas as large as 1000m^2 per gram of material, see [22], [29], [30], and [31]. In this context the solvent is the scarce minority phase, whose volume is restricted by the elastic nature of the polymer electrolyte matrix which resists swelling.

In a biological setting amphiphilic materials include lipids, small bi-phasic molecules with a polar head group which attracts a hydration sphere of solvent molecules and a "greasy" or "hydrophobic" tail which mixes poorly with solvent. The hydrophobic groups agglomerate with the polar head-groups pointing outwards so as to interact with the solvent, while the hydrophobic tails lie in a solvent-excluded region. The classic morphology is the bilayer membrane, in which two sheets of lipids align along a co-dimension one hypersurface.When the center-line hypersurface is closed, the resulting structure is called a liposome or vesicle. However the lipids can also assemble into cylindrical pore-like structures, or into spherical micelles with the tails filling the interior, see Figure **??**.

In recent work, Budin and Szostak [1] investigated the dynamics and division of primitive cellular membranes, comprised primarily of single-chain lipids. They describe the so-called "phospholipid war" in which cells with higher concentrations of phospholipids are more successful in attracting and retaining lipids from the ambient environment. They propose that the resulting selective advantage would drive cells to maximize their phospholipid content, leading them to more closely resemble

---

*Department of Mathematical Sciences, New Mexico State University, Las Cruces, NM 88003, USA (`sdai@nmsu.edu`)

†Department of Mathematics, Michigan State University, East Lansing, MI 48824, USA (`kpromisl@math.msu.edu`)

modern cellular membranes. They also propose a route for cell division in primitive cells via the bifurcation of spherical bilayer (liposome) into cylindrical pores, which they induce by varying the concentration free lipids within the solvent phase. Similar budding bifurcations in amphiphilic diblock copolymers are obtained by varying surfactant concentrations, see Figure 1 of [33]. Motivated in part by these experiments we derive a curvature driven sharp-interface flow for closed cylindrical pores under the functionalized Cahn-Hilliard gradient flow, and investigate the *competitive* geometric evolution of co-existing liposomes (closed bilayers) with closed cylindrical pores. Our central result describes the role that the 'background' or 'far-field' value of the surfactant phase residing within the dominant phase has on the competitive evolution of distinct morphologies, particularly bilayer and pore structures.

1.1. Description of the functionalized Cahn Hilliard free energy. The functionalized Cahn-Hilliard (FCH) free energy models the free energy of a binary mixture of a surfactant phase and a solvent. It incorporates hydrophilic interactions by lowering the free energy in response to the creation of surfactant-wetted surface area, however it respects the molecular structure of the surfactant phase by penalizing surfactant interfaces which are too thin. The FCH free energy is a reformulation of the classical Cahn-Hilliard free energy, [2],

$$\mathcal{E}(u) = \int_\Omega \frac{\varepsilon^2}{2} |\nabla u|^2 + W(u) \, dx \tag{1.1}$$

which assigns energy to binary mixtures over a domain $\Omega \subset \mathbb{R}^3$ in terms of the volume fraction $u \in H^1(\Omega)$. The mixing potential $W : \mathbb{R} \mapsto \mathbb{R}$ describes the compatibility of the two phases, and is assumed to have two successive local minima at $b_- < b_+$ with *unequal* depths $W(b_-) = 0 > W(b_+)$, and a transverse intermediate zero at $u_m \in (b_-, b_+)$. Morever we assume the minima are non-degenerate, with $\alpha_\pm := W''(b_\pm) > 0$.

The Cahn-Hilliard free energy supports many critical points which are zeros of the $L^2(\Omega)$ variational derivative of the Cahn-Hilliard energy

$$\frac{\delta \mathcal{E}}{\delta u}(u) := -\varepsilon^2 \Delta u + W'(u) = 0. \tag{1.2}$$

When subject to a total mass constraint

$$\int_\Omega u \, dx = M, \tag{1.3}$$

for a prescribed $M \in \mathbb{R}$, the local minimizers of the Cahn-Hilliard free energy include single-layer interfaces, U_s, which separate bulk phases of $u = b_-$ from $u = b_+$ across an order of ε width interface. At leading order the single layer interface solves the one-dimensional equilibrium equation

$$\partial_z^2 U_s = W'(U_s) + \lambda, \tag{1.4}$$

where z is ε-scaled distance to the mid-point of the interface and the Lagrange multiplier λ, dual to the mass constraint, takes the critical value for which (1.4) supports a heteroclinic connection. However the Cahn-Hilliard free energy also supports a wide variety of *saddle point* structures, among these are *bilayer interfaces* U_b which solve

$$\partial_z^2 U_b = W'(U_b), \tag{1.5}$$

2

subject to the homoclinic conditions, $U = b_-$ at $z = \pm\infty$. These interfaces are also order of ε in width but separate two regions of $u = b_-$ by a thin co-dimension one surface on which u approaches the intermediate zero, $u = u_m \in (b_-, b_+)$, of W. Saddle point structures can also be formed from cylindrically symmetric critical points, which we term *pore solutions*. Indeed, fixing a co-dimension two interface, Γ_p, which defines the center-line of the pore structure, and introducing R, the ε scaled radial distance to a Γ_p, the associated pore profile U_p solves the radial version of (1.2),

$$\partial_R^2 U_p + \frac{1}{R}\partial_R U_p = W'(U_p), \qquad (1.6)$$

subject to the boundary conditions $\partial_R U_p(0) = 0$ and $U_p \to b_-$ as $R \to \infty$. The saddle point structures of $\mathcal{E}$ have compelling agreement with the morphologies generated by amphiphilic mixtures, see [20], [21], and [33] for experimental examples, in particular they possess a very large ratio of surface area to volume of minority phase. However the large surface area saddle-point structures are wildly unstable under gradient flows of the Cahn-Hilliard energy.

The functionalized Cahn-Hilliard free energy, proposed in [13], stabilizes the high-surface area saddle point structures of the Cahn-Hillard energy. It takes the form

$$\mathcal{F}(u) := \int_\Omega \frac{1}{2}\left(\frac{\delta\mathcal{E}}{\delta u}\right)^2 - \varepsilon^2\left(\eta_1\frac{\varepsilon^2}{2}|\nabla u|^2 + \eta_2 P(u)\right)dx, \qquad (1.7)$$

and is naturally considered subject to a constraint on total mass over a function space $H_N^2(\Omega)$ where the N subscript denotes zero-flux boundary conditions, such as periodic or homogeneous Neumann ($\vec{n} \cdot \nabla u = 0$ on $\partial\Omega$). The dominant term in the FCH free energy, referred to loosely as the Willmore contribution, is the square of the $L^2(\Omega)$ variational derivative of the Cahn-Hilliard energy given in (1.2). The Willmore contribution is minimized at *any* critical point of the Cahn-Hilliard energy; the functionalization terms, multiplied by the ε^2 prefactor, perturbatively reward critical points of $\mathcal{E}$ with "desirable" features. There are two natural scalings for the prefactor: the weak functionalization, taken here and in Γ-limit scalings, selects an ε^2 prefactor which balances with the $O(\varepsilon)$ residuals appearing in $\frac{\delta\mathcal{E}}{\delta u}$. This scaling leads to morphological competition on the $O(\varepsilon^{-2})$ time scale which is nonlinear in curvature. The strong functionalization, considered in [9] sets the perturbation prefactor as ε, so that the functionalization terms dominate the Willmore residual, leading to a morphological competition on the $O(\varepsilon^{-1})$ time-scale which is linear in curvature.

For $\eta_1 > 0$, the first functionalization term assigns lower free energy to critical point structures of the Cahn-Hilliard free energy with large surface area. As a model of amphiphilic mixtures, this corresponds to the energetic preference for the surfactant phase to spread out in a thin interfacial layer whose extend is constrained by the volume of surfactant and by their molecular width, [14]. Within the framework of the FCH free energy, the molecular width is described by the width of the bilayer, U_b, and pore, U_p, profiles. The second perturbative term incorporates pressure jumps between solvent and surfactant phases, which are taken to depend upon mixture concentrations through a multiple, $\eta_2 \in \mathbb{R}$, of the capillary pressure $P = P(u)$. In the sequel we choose the functional form $P(u) = W(u)$ for convenience, as it simplifies the evaluation of several integrals, see [14] for further discussion of the molecular origins of the pressure term. A related free energy expression for amphiphilic mixtures was derived in [15] from an examination of the small angle x-ray scattering (SAXS) data, with the primarily distinction being that the well, W, was piece-wise linear.

3

Single layer interfaces have been employed to describe a wide range of physical phenomena. Higher order free energies, similar to the FCH with the significant exception that $\eta_1 < 0$ and the mixing well W is untitled, have been proposed, see [23] and [32]. Indeed, the De Giorgi conjecture, which concerns the Γ limit of the FCH energy for $\eta_1 < 0$ with an untilted well has been established, [28]. Extensions of these models to address deformations of elastic vesicles subject to volume constraints, [11], and multicomponent models which incorporate a variable intrinsic curvature have been investigated, [24]. However, the single-layer interface forms the essential underpinning of each of these models. For amphiphilic materials, with $\eta_1 > 0$ the FCH energy landscape is fundamentally different. Indeed, for fixed $\varepsilon > 0$ the FCH energy is bounded below and has global minimizers, see [27], *however* for $\eta_1 > 0$ the lower bound tends to $-\infty$ as $\varepsilon \to 0^+$ for fixed volume fraction. A Γ-limit analysis of the FCH will require new ideas, particularly since defect structures, such as end-caps and junctions, may form spatially dense sets as $\varepsilon \to 0^+$.

1.2. Main Results. This paper addresses the competitive evolution of bilayer and pore structures under the Functionalized Cahn-Hilliard equation: the H^{-1} gradient flow of the FCH energy

$$u_t = \Delta \overbrace{\left\{\left(-\varepsilon^2\Delta + W''(u) - \varepsilon^2\eta_1\right)\left(-\varepsilon^2\Delta u + W'(u)\right) + \varepsilon^2(\eta_1 - \eta_2)W'(u)\right\}}^{\mu := \frac{\delta\mathcal{F}}{\delta u}}, \quad (1.8)$$

over a function space $H_N^6(\Omega)$ where the N subscript denotes zero-flux boundary conditions, such as periodic or homogeneous Neumann ($\vec{n} \cdot \nabla u = \vec{n} \cdot \nabla\Delta u = \vec{n} \cdot \nabla\mu = 0$ on $\partial\Omega$) boundary conditions.

We consider the evolution of a disjoint family of co-dimension one bilayer morphologies, with center-line hypersurface $\Gamma_b \subset \mathbb{R}^3$ together with a disjoint family of co-dimension two pore morphologies, with center-curve $\Gamma_p \subset \mathbb{R}^3$, which are far from self-intersection, or from intersecting each other, as measured in the ε-scaled distance. A key result is that, away from the interfaces, the chemical potential is spatially constant,

$$\mu(t) := \mu_0 + \varepsilon\mu_1(t) + \varepsilon^2\mu_2(t) + O(\varepsilon^3),$$

and moreover the competitive evolution of the interfaces is mediated through this far-field value of the chemical potential, which we show is proportional to the density of surfactant (lipids) in the bulk (solvent) phase. We say that the interfaces Γ_b and Γ_p are at *quasi-equilibrium* if their dynamics are at equilibrium on the $O(\varepsilon^{-1})$ time-scale, equivalently if $\mu_0 = \mu_1 = 0$, see (5.41) and (1.7)-(1.8) of [8].

In [8] we derived the evolution of a disjoint family of closed, co-dimension one bilayers interfaces in $\mathbb{R}^n$. On the $t_2 := \varepsilon^2 t$ time-scale, the interface Γ_b evolves according to a Willmore-type flow with normal velocity prescribed by

$$V_b = \frac{\sigma_b}{m_b}\left(\Delta_s + K - \frac{1}{2}H^2 + \frac{\eta_1 + \eta_2}{2} + \lambda_b\mu_2\right)H, \quad (1.9)$$

where for $n = 3$, the total and quadratic curvatures $H = k_1 + k_2$ and $K = k_1^2 + k_2^2$, are defined in terms of the principle curvatures $k_i, i = 1, 2$ of Γ_b. The operator Δ_s is the Laplace-Beltrami operator associated to Γ_b, and

$$m_b := \int_{\mathbb{R}} \hat{U}_b(z)\,dz, \qquad \lambda_b := \frac{2m_b}{\int_{\mathbb{R}} |\hat{U}_b'|^2\,dz}, \qquad \sigma_b := \frac{m_b \int_{\mathbb{R}} |\hat{U}_b'|^2\,dz}{\int_{\mathbb{R}} |\hat{U}_b|^2\,dz}, \quad (1.10)$$

4

are positive constants determined solely by the double well potential W in the FCH energy through the bilayer profile $\hat{U}_b := U_b - b_-$. In particular m_b denotes the mass of surfactant per unit area of bilayer. For single-layer interfaces, the interface evolution is governed by a Mullins-Sekerka flow, as in [25]. For bilayers the Mullins-Sekerka problem is trivial, leading to a spatially constant chemical potential, $\mu_2 = \mu_2(t_2)$, whose value is determined by conservation of total mass. The end result is an *interfacial-area preserving* Willmore flow: the collection of bilayers evolves under (1.9) with μ_2 determined so that the total surface area is unchanged.

In this work, we first establish the geometric evolution of a collection of disjoint closed-loop pores in $\mathbb{R}^3$, characterized by a co-dimension two interface Γ_p. Subsequently we show that the geometric evolution of co-existing pore and bilayer structures is mediated through the common value of the far-field chemical potential, $\mu_2 = \mu_2(t_2)$, which is proportional to the ambient level of surfactant phase in the solvent domain. Our results are formal, and in particular we assume that the bilayer and pore profiles are stable. It is known that the sole mechanism for linear instability of a bilayer interface is through high-frequency, in-plane modulations of the bilayer width, called a pearling instability, [17], detailed conditions under which the pearling instability are manifest have been determined for both the strong and weak functionalization, [9, 10].

THEOREM 1.1. *We assume that the pore and bilayer morphologies are stable with respect to the pearling instability. Then on the slow, $t_2 = \varepsilon^2 t$ time-scale the evolution of well-separated, quasi-equilibrium bilayer and pore structures, with center interface Γ_b and center line Γ_p, is given by (1.9) coupled to the vector normal velocity of pore structures*

$$\mathbf{V}_p = -\frac{\sigma_p}{m_p}\left(\partial_s^2 + \frac{1}{4}|\vec{\kappa}|^2 + \eta_1 + \lambda_p\mu_2\right)\vec{\kappa}, \tag{1.11}$$

where $m_p := 2\pi S_1$, the mass per unit length of pore, and the positive constants $\sigma_p := 2\pi S_1 S_4/S_2$ and $\lambda_p := 2S_1/S_4$ depend upon the double well, W, through the pore profile, U_p, defined in (1.6), via the relations (4.23) and (6.24). The vector normal velocity $\mathbf{V}_p$ and vector curvature $\vec{\kappa} = (\kappa_1, \kappa_2)^t$ are taken in the coordinate system of Lemma 2.2, see also (6.34). The coupling between the bilayer and pore morphologies is through the spatially constant value of $\mu_2 = \mu_2(t_2)$, which is determined from the mass constraint

$$0 = m_b\frac{d}{dt}|\Gamma_b| + m_p\varepsilon\frac{d}{dt}|\Gamma_p| = m_b\int_{\Gamma_b}V_b(S)H(S)\,dS - m_p\varepsilon\int_{\Gamma_p}\mathbf{V}_p(s)\cdot\vec{\kappa}(s)\,ds. \tag{1.12}$$

For a collection of spherical bilayers and circular pores the evolution reduces to system of ODEs for the radii given by (7.10)-(7.11) coupled through (7.12). In particular if the bifurcation parameter,

$$\nu := (\lambda_p - 2\lambda_b)\eta_1 + \lambda_p\eta_2, \tag{1.13}$$

satisfies $\nu < 0$, then the circular pores will grow until the spherical bilayers extinguish, while if $\nu > 0$ then there are asymptotically stable configurations of coexisting circular pores with common radius and spherical bilayers with arbitrary radii.

In section 2 we establish the coordinate system for the co-dimension two structures and introduce the near and far field expansions for the chemical potentials and pore profile. In section 3 we address the relaxation of the FCH equation for initial

data in the neighborhood of a pore structure, on the fast $T_2 = t/\varepsilon^2$ time scale. In section 4 we address the $t = O(1)$ time scale, deriving a free surface problem which possesses spatially constant outer solutions. In section 5 we address the $t_1 = \varepsilon t$ time-scale, deriving a coupled system, (5.31) and (5.41), for the normal velocity and far-field chemical potential. The curvature driven flow is quenched by the chemical potential, whose expression of mass conservation serves to arrest the flow, driving it to equilibria. In section 6 we analyze the $t_2 = \varepsilon^2 t$ time-scale, deriving the length-preserving Wilmoresque flow (6.45) for well-separated, closed-loop pores. In section 7 we couple the evolution of the closed-loop pores to that of bilayers derived in [8]. The resulting evolution, coupled through the mass constraint (1.12), is further reduced and analyzed for the special case of spherical bilayers and circularly symmetric pore structures.

2. Moving frame, inner expansion, and normal derivatives. We first address the co-dimension two structures. We consider a smooth, closed curve, $\Gamma \subset \mathbb{R}^3$ parameterized by ϕ

$$\Gamma(t) = \left\{ \phi(s,t) : [0, L(t)] \times [0, T] \mapsto \mathbb{R}^3 \,\middle|\, \phi(0,t) = \phi(L(t),t)) \right\}, \qquad (2.1)$$

where s denotes arc-length and $L = L(t)$ is the total curve length. At a given point on Γ, the unit tangent vector $\mathbf{T}$, the principal normal vector $\mathbf{N}$ and the binormal vector $\mathbf{B}$ defined by

$$\mathbf{T} = \frac{\partial \phi}{\partial s}, \quad \mathbf{N} = \left\| \frac{\partial \mathbf{T}}{\partial s} \right\|^{-1} \frac{\partial \mathbf{T}}{\partial s}, \quad \mathbf{B} = \mathbf{T} \times \mathbf{N}, \qquad (2.2)$$

form the Frenet-Serret frame. For fixed t the vectors are coupled via the curvature, κ, and torsion τ of the curve, The Frenet-Serret formulas are

$$\frac{\partial \mathbf{T}}{\partial s} = \kappa \mathbf{N}, \qquad (2.3)$$

$$\frac{\partial \mathbf{N}}{\partial s} = -\kappa \mathbf{T} + \tau \mathbf{B}, \qquad (2.4)$$

$$\frac{\partial \mathbf{B}}{\partial s} = -\tau \mathbf{N}. \qquad (2.5)$$

The $\{\mathbf{T}, \mathbf{N}, \mathbf{B}\}$ coordinate system is not convenient for our calculations due to the asymmetry of the roles played by $\mathbf{N}$ and $\mathbf{B}$. To circumvent this, we define a new coordinate system, $\{\mathbf{T}, \mathbf{N}^1, \mathbf{N}^2\}$ such that at each point $\phi(s,t)$ on the curve $\Gamma(t)$ the vectors $\{\mathbf{N}^1, \mathbf{N}^2\}$ form an orthonormal basis for the normal plane and

$$\frac{\partial \mathbf{N}^i}{\partial s} = -\kappa_i \mathbf{T}, \quad i = 1, 2, \qquad (2.6)$$

where $\vec{\kappa}(s,t) := (\kappa_1, \kappa_2)^t$ is the normal curvature vector with respect to $\{\mathbf{N}^1, \mathbf{N}^2\}$. The same orthonormal basis has been used by Calini and Ivey for the study of the motion of thin vortex filaments in an ideal fluid [3]. Here we include an existence result in the general setting.

LEMMA 2.1. *Let $M \in \mathbb{R}^{2 \times 2}$ satisfy the differential equation*

$$\frac{d}{ds} M(s) = \begin{pmatrix} 0 & \tau(s) \\ -\tau(s) & 0 \end{pmatrix} M(s), \qquad (2.7)$$

subject to initial data $M(0) = M_0$. If M_0 is orthonormal, then so is M and the vectors $\{\mathbf{N}^1, \mathbf{N}^2\}$ defined by

$$\left(\mathbf{N}^1(s), \mathbf{N}^2(s)\right) := \left(\mathbf{N}(s), \mathbf{B}(s)\right)M(s), \tag{2.8}$$

form an orthonormal basis for the normal plane and satisfy (2.6) with

$$\kappa_i(s) = M_{1i}(s)\kappa(s), \tag{2.9}$$

for $i = 1, 2..$

Proof. Let the initial data M_0 be an orthonormal matrix, and let M be the corresponding solution of (2.7). We observe that $\frac{d}{ds}(M^t M) = 0$ and since $M_0^t M_0 = I$, we have $M^t M = I$ for all s, that is, $M(s)$ is orthonormal. The vectors $\{\mathbf{N}^1, \mathbf{N}^2\}$ defined by (2.8) are orthonormal and lie in the normal plane to Γ at s, hence they span the plane. In addition, taking ∂_s of (2.8) and using the Frenet relations (2.3)-(2.5) and (2.6) we find

$$\begin{aligned}
\frac{\partial \mathbf{N}^i}{\partial s} &= M'_{1i}\mathbf{N} + M'_{2i}\mathbf{B} + M_{1i}\frac{\partial \mathbf{N}}{\partial s} + M_{2i}\frac{\partial \mathbf{B}}{\partial s}, \\
&= \tau M_{2i}\mathbf{N} - \tau M_{1i}\mathbf{B} + M_{1i}\left(-\kappa\mathbf{T} + \tau\mathbf{B}\right) - M_{2i}\tau\mathbf{N} = -\kappa_i\mathbf{T},
\end{aligned}$$

which establishes (2.6) for κ_i defined in (2.9). $\square$

We define the normal velocity $\mathbf{V} = (V_1, V_2)^t$ of the point $\phi(s, t)$ on $\Gamma(t)$ via

$$V_i := \mathbf{N}^i \cdot \frac{\partial \phi}{\partial t}(s, t), \tag{2.10}$$

for $i = 1, 2$. The following lemma demonstrates the utility of the $\{\mathbf{T}, \mathbf{N}^1, \mathbf{N}^2\}$ coordinates.

LEMMA 2.2. *The $\{\mathbf{T}, \mathbf{N}^1, \mathbf{N}^2\}$ coordinate system satisfies*

$$\frac{\partial \mathbf{T}}{\partial s} = \kappa_1\mathbf{N}^1 + \kappa_2\mathbf{N}^2, \tag{2.11}$$

while the curve length evolves according to

$$\frac{d|\Gamma|}{dt} = -\int_\Gamma \mathbf{V} \cdot \vec{\kappa} \, ds. \tag{2.12}$$

Proof. Taking ∂_s of $\mathbf{T} \cdot \mathbf{T} = 1$ we see that $\frac{\partial \mathbf{T}}{\partial s} \cdot \mathbf{T} = 0$ and hence $\frac{\partial \mathbf{T}}{\partial s} = a_1(s)\mathbf{N}^1 + a_2(s)\mathbf{N}^2$ for some functions $a_1(s), a_2(s)$. Moreover, taking ∂_s of $0 = \mathbf{T} \cdot \mathbf{N}^i$, we arrive at the relation

$$0 = \frac{\partial \mathbf{T}}{\partial s} \cdot \mathbf{N}^i + \mathbf{T} \cdot \frac{\partial \mathbf{N}^i}{\partial s} = a_i(s) - \kappa_i, \tag{2.13}$$

and hence $a_i = \kappa_i$.

To calculate the change in curve length it is convenient to parametrize the family of curves $\{\Gamma(t) : t_0 - \delta < t < t_0 + \delta\}$ by a common parameter $\xi \in [a, b]$:

$$\Gamma(t) = \{\gamma(\xi, t) : \xi \in [a, b]\} \quad \text{for all } t \in (t_0 - \delta, t_0 + \delta). \tag{2.14}$$

We take ξ to be arc length parameter at $t = t_0$. It follows that

$$|\Gamma(t)| = \int_a^b \left\|\frac{\partial \gamma}{\partial \xi}(\xi, t)\right\| \, d\xi,$$

and taking the time derivative we find

$$\frac{d|\Gamma|}{dt} = \int_a^b \frac{\partial}{\partial t}\left\|\frac{\partial\gamma}{\partial\xi}(\xi,t)\right\| d\xi = \int_a^b \left\|\frac{\partial\gamma}{\partial\xi}(\xi,t)\right\|^{-1}\frac{\partial\gamma}{\partial\xi}\cdot\frac{\partial^2\gamma}{\partial\xi\partial t} d\xi$$

$$= -\int_a^b \frac{\partial}{\partial\xi}\left(\left\|\frac{\partial\gamma}{\partial\xi}(\xi,t)\right\|^{-1}\frac{\partial\gamma}{\partial\xi}\right)\cdot\frac{\partial\gamma}{\partial t} d\xi, \tag{2.15}$$

where the boundary terms canceled in the integration by parts since $\Gamma(t)$ is smooth and closed. Since ξ corresponds to arc length at $t = t_0$, we have

$$\frac{\partial\gamma}{\partial\xi}(\xi,t_0) = \mathbf{T}, \quad \left\|\frac{\partial\gamma}{\partial\xi}(\xi,t_0)\right\| = 1, \tag{2.16}$$

and substituting $t = t_0$ in (2.15) yields

$$\frac{d|\Gamma|}{dt}(t_0) = -\int_a^b \frac{\partial\mathbf{T}}{\partial\xi}\cdot\frac{\partial\gamma}{\partial t} d\xi = -\int_a^b (\kappa_1\mathbf{N}^1 + \kappa_2\mathbf{N}^2)\cdot\frac{\partial\gamma}{\partial t} d\xi,$$

$$= -\int_a^b (\kappa_1 V_1 + \kappa_2 V_2) d\xi = -\int_\Gamma (\kappa_1 V_1 + \kappa_2 V_2) ds. \tag{2.17}$$

☐

Assuming that Γ is smooth, then from the Implicit Function theorem there is a neighborhood $\Gamma_\ell \subset \mathbb{R}^3$ of Γ such that each $x \in \Gamma_\ell$ can be uniquely represented as

$$x = \phi(s,t) + r_1\mathbf{N}^1(s,t) + r_2\mathbf{N}^2(s,t) \tag{2.18}$$

where $s = s(x,t)$ and $\vec{r} = (r_1(x,t), r_2(x,t))$ are as smooth as γ'. In the rescaled normal coordinates $z = (z_1, z_2)^t := \varepsilon^{-1}\vec{r}$ we have the following identities.

LEMMA 2.3. *Fix Γ and assume that ℓ is so small that $\|\vec{\kappa}\|_{L^\infty(\Gamma)}\ell < 1$. Then on Γ_ℓ, the change of variables $(x,t) \mapsto (s,z,t)$ transforms the Cartesian Laplacian to*

$$\Delta_x = \varepsilon^{-2}\Delta_z - \varepsilon^{-1}\frac{\vec{\kappa}}{1 - \varepsilon z\cdot\vec{\kappa}}\cdot\nabla_z + \frac{1}{(1 - \varepsilon z\cdot\vec{\kappa})^2}\partial_s^2 + \frac{\varepsilon z\cdot\partial_s\vec{\kappa}}{(1 - \varepsilon z\cdot\vec{\kappa})^3}\partial_s, \tag{2.19}$$

while the normal velocity $\mathbf{V}$ takes the form

$$V_1 = -\varepsilon\frac{\partial z_1}{\partial t} + \varepsilon z_2\mathbf{N}^2\cdot\frac{\partial\mathbf{N}^1}{\partial t}, \tag{2.20}$$

$$V_2 = -\varepsilon\frac{\partial z_2}{\partial t} + \varepsilon z_1\mathbf{N}^1\cdot\frac{\partial\mathbf{N}^2}{\partial t}. \tag{2.21}$$

Moreover the Jacobian associated to the change of variables takes the form

$$J(s,z) = \varepsilon^2 - \varepsilon^3 z\cdot\vec{\kappa}. \tag{2.22}$$

Proof. The relation (2.19) follows from a standard calculation. To obtain the normal velocity expressions we re-write (2.18) as

$$\varepsilon z_1(x,t) = (x - \phi(s,t))\cdot\mathbf{N}^1(s,t), \quad \varepsilon z_2(x,t) = (x - \phi(s,t))\cdot\mathbf{N}^2(s,t). \tag{2.23}$$

Taking ∂_t of the z_1 equation we find

$$\varepsilon\frac{\partial z_1}{\partial t} = \left(-\frac{\partial\phi}{\partial s}\frac{\partial s}{\partial t} - \frac{\partial\phi}{\partial t}\right)\cdot\mathbf{N}^1 + (x - \phi(s,t))\cdot\left(\frac{\partial\mathbf{N}^1}{\partial s}\frac{\partial s}{\partial t} + \frac{\partial\mathbf{N}^1}{\partial t}\right)$$

8

$$= \left(-\mathbf{T}\frac{\partial s}{\partial t} - \frac{\partial \phi}{\partial t} \right) \cdot \mathbf{N}^1 + \varepsilon(z_1\mathbf{N}^1 + z_2\mathbf{N}^2) \cdot \left(-\kappa_1\mathbf{T}\frac{\partial s}{\partial t} + \frac{\partial \mathbf{N}^1}{\partial t} \right)$$

$$= -\frac{\partial \phi}{\partial t} \cdot \mathbf{N}^1 + \varepsilon z_2\mathbf{N}^2 \cdot \frac{\partial \mathbf{N}^1}{\partial t}. \tag{2.24}$$

The relations (2.10) yield (2.20), and the derivation of (2.21) is similar. The Jacobian matrix takes the form

$$\mathbf{J} = \frac{\partial x}{\partial(s, z_1, z_2)} = \left((1 - \varepsilon z_1\kappa_1 - \varepsilon z_2\kappa_2)\mathbf{T}, \varepsilon\mathbf{N}^1, \varepsilon\mathbf{N}^2 \right), \tag{2.25}$$

and evaluating the determinant yields (2.22). □

REMARK 2.4. *The terms $z_2\mathbf{N}^2 \cdot \frac{\partial \mathbf{N}^1}{\partial t}$ and $z_1\mathbf{N}^1 \cdot \frac{\partial \mathbf{N}^2}{\partial t}$ in (2.20) and (2.21) reflect lower order contributions to the normal velocity induced by the rotational motion of the curve $\Gamma(t)$.*

For notational convenience we introduce

$$\Delta_0 := \frac{\partial^2}{\partial s^2} - (z \cdot \vec{\kappa})\vec{\kappa} \cdot \nabla_z, \tag{2.26}$$

are rewrite the Cartesian Laplacian expansion, (2.19) in the more compact form

$$\Delta_x = \varepsilon^{-2}\Delta_z - \varepsilon^{-1}\vec{\kappa} \cdot \nabla_z + \Delta_0 + \varepsilon\Delta_1 + O(\varepsilon^2), \tag{2.27}$$

where the precise form of Δ_1 and lower order terms is immaterial for the analysis. Considering a time scale $\hat{t}$, we have the formal inner expansion of a quantity v

$$v(x, t) = \tilde{v}(s, z, t) = \tilde{v}_0 + \varepsilon\tilde{v}_1 + \varepsilon^2\tilde{v}_2 + \varepsilon^3\tilde{v}_3 + O(\varepsilon^4), \tag{2.28}$$

where $\tilde{v}_i = \tilde{v}_i(s, z, \hat{t})$. The Cartesian Laplacian of v then admits the inner expansion

$$\Delta_x v = \varepsilon^{-2}\Delta_z\tilde{v} - \varepsilon^{-1}\vec{\kappa} \cdot \nabla_z\tilde{v} + \Delta_0\tilde{v} + O(\varepsilon)$$
$$= \varepsilon^{-2}\Delta_z\tilde{v}_0 + \varepsilon^{-1}\left(\Delta_z\tilde{v}_1 - \vec{\kappa} \cdot \nabla_z\tilde{v}_0 \right) + \left(\Delta_z\tilde{v}_2 - \vec{\kappa} \cdot \nabla_z\tilde{v}_1 + \Delta_0\tilde{v}_0 \right)$$
$$+ \varepsilon\left(\Delta_z\tilde{v}_3 - \vec{\kappa} \cdot \nabla_z\tilde{v}_2 + \Delta_0\tilde{v}_1 + \Delta_1\tilde{v}_0 \right) + O(\varepsilon^2). \tag{2.29}$$

To develop an inner expansion for the chemical potential, μ, we substitute the inner expansion (2.28) of u into (1.8), obtaining

$$\mu(x, t) = \left(-\varepsilon^2\Delta_x + W''(u) - \varepsilon^2\eta_1 \right)\left(-\varepsilon^2\Delta_x u + W'(u) \right) + \varepsilon^2(\eta_1 - \eta_2)W'(u)$$

$$= \left[-\Delta_z + W''(\tilde{u}_0) + \varepsilon\left(\vec{\kappa} \cdot \nabla_z + W'''(\tilde{u}_0)\tilde{u}_1 \right) \right.$$

$$+ \varepsilon^2\left(-\Delta_0 + W'''(\tilde{u}_0)\tilde{u}_2 + W^{(4)}(\tilde{u}_0)\frac{\tilde{u}_1^2}{2} - \eta_1 \right)$$

$$\left. + \varepsilon^3\left(-\Delta_1 + W'''(\tilde{u}_0)\tilde{u}_3 + W^{(4)}(\tilde{u}_0)\tilde{u}_1\tilde{u}_2 + \frac{1}{6}W^{(5)}(\tilde{u}_0)\tilde{u}_1^3 \right) + O(\varepsilon^4) \right]$$

$$\cdot \left[\left(-\Delta_z\tilde{u}_0 + W'(\tilde{u}_0) \right) + \varepsilon\left(-\Delta_z\tilde{u}_1 + \vec{\kappa} \cdot \nabla_z\tilde{u}_0 + W''(\tilde{u}_0)\tilde{u}_1 \right) \right.$$

$$+ \varepsilon^2\left(-\Delta_z\tilde{u}_2 + \vec{\kappa} \cdot \nabla_z\tilde{u}_1 - \Delta_0\tilde{u}_0 + W''(\tilde{u}_0)\tilde{u}_2 + \frac{1}{2}W'''(\tilde{u}_0)\tilde{u}_1^2 \right)$$

$$+ \varepsilon^3\left(-\Delta_z\tilde{u}_3 + \vec{\kappa} \cdot \nabla_z\tilde{u}_2 - \Delta_0\tilde{u}_1 - \Delta_1\tilde{u}_0 + W''(\tilde{u}_0)\tilde{u}_3 \right.$$

9

$$\left. + W'''(\tilde{u}_0)\tilde{u}_1\tilde{u}_2 + \frac{1}{6}W^{(4)}(\tilde{u}_0)\tilde{u}_1^3\right) + O(\varepsilon^4)\right]$$
$$+ \varepsilon^2(\eta_1 - \eta_2)W'(\tilde{u}_0) + \varepsilon^3(\eta_1 - \eta_2)W''(\tilde{u}_0)\tilde{u}_1 + O(\varepsilon^4). \tag{2.30}$$

Thus the chemical potential admits an inner expansion of the form (2.28) where

$$\tilde{\mu}_0 = \left(-\Delta_z + W''(\tilde{u}_0)\right)\left(-\Delta_z\tilde{u}_0 + W'(\tilde{u}_0)\right), \tag{2.31}$$

$$\tilde{\mu}_1 = \left(-\Delta_z + W''(\tilde{u}_0)\right)\left(-\Delta_z\tilde{u}_1 + \vec{\kappa}\cdot\nabla_z\tilde{u}_0 + W''(\tilde{u}_0)\tilde{u}_1\right)$$
$$+ \left(\vec{\kappa}\cdot\nabla_z + W'''(\tilde{u}_0)\tilde{u}_1\right)\left(-\Delta_z\tilde{u}_0 + W'(\tilde{u}_0)\right), \tag{2.32}$$

$$\tilde{\mu}_2 = \left(\Delta_z - W''(\tilde{u}_0)\right)\left(\Delta_z\tilde{u}_2 - \vec{\kappa}\cdot\nabla_z\tilde{u}_1 + \Delta_0\tilde{u}_0 - W''(\tilde{u}_0)\tilde{u}_2 - \frac{W'''(\tilde{u}_0)\tilde{u}_1^2}{2}\right)$$
$$+ \left(\vec{\kappa}\cdot\nabla_z + W'''(\tilde{u}_0)\tilde{u}_1\right)\left(-\Delta_z\tilde{u}_1 + \vec{\kappa}\cdot\nabla_z\tilde{u}_0 + W''(\tilde{u}_0)\tilde{u}_1\right)$$
$$+ \left(-\Delta_0 + W'''(\tilde{u}_0)\tilde{u}_2 + W^{(4)}\frac{\tilde{u}_1^2}{2} - \eta_1\right)\left(-\Delta_z\tilde{u}_0 + W'(\tilde{u}_0)\right)$$
$$+ (\eta_1 - \eta_2)W'(\tilde{u}_0). \tag{2.33}$$

The quantity $\tilde{\mu}_3$ is relevant to the asymptotic results we develop, however we derive its form under the simplification, $\tilde{u}_1 = 0$, in (2.30).

A key step in the analysis is the matching conditions between the inner and outer solutions. The outer problem is posed on a domain $\Omega\backslash\Gamma$ with a co-dimension two boundary, accordingly the proper treatment of the matching conditions requires a careful development of the definition of the normal derivatives at the interface Γ. Fixing $x = \phi(s) \in \Gamma$ we take two unit vectors $\mathbf{n}, \mathbf{m} \in \text{span}\{\mathbf{N}^1(x), \mathbf{N}^2(x)\}$ in the normal plane of Γ at x, and further specify that $\mathbf{n} = \cos(\theta)\mathbf{N}^1 + \sin(\theta)\mathbf{N}^2$. The usual directional derivative along $\mathbf{n}$ is denoted

$$\partial_\mathbf{n} := \mathbf{n}\cdot\nabla_x = \cos\theta\,\mathbf{N}^1\cdot\nabla_x + \sin\theta\,\mathbf{N}^2\cdot\nabla_x, \tag{2.34}$$

and for $f \in \mathcal{C}^\infty(\Omega\backslash\Gamma)$ we introduce the $\mathbf{n}, \mathbf{m}$ limit

$$\partial_\mathbf{n}^j f^\mathbf{m}(x) := \lim_{h\to0^+} (\mathbf{n}\cdot\nabla_x)^j f(x + h\mathbf{m}, t) \quad \text{for all } j \geq 0, \tag{2.35}$$

and the limit of the gradient

$$\nabla_x f^\mathbf{m}(x) := \lim_{h\to0^+} \nabla_x f(x + h\mathbf{m}, t), \tag{2.36}$$

where the limits exist. If $f \in C^1(\Omega)$ then the normal derivative of f will satisfy $\partial_\mathbf{n} f^{-\mathbf{m}} = \partial_\mathbf{n} f^\mathbf{m}$. This motivates the following definition of the jump condition:

$$[\partial_\mathbf{n} f^\mathbf{n}]_\Gamma(x) := \partial_\mathbf{n} f^\mathbf{n}(x) - \partial_\mathbf{n} f^{-\mathbf{n}}(x), \tag{2.37}$$

which is zero when f has a smooth extension through Γ.

With this notation we examine the matching condition

$$(\mu_0 + \varepsilon\mu_1 + \varepsilon^2\mu_2 + \dots)(x + \varepsilon R\mathbf{n}, t) \approx (\tilde{\mu}_0 + \varepsilon\tilde{\mu}_1 + \varepsilon^2\tilde{\mu}_2 + \dots)(s, R, \theta, t) \tag{2.38}$$

as εR becomes $o(1)$. Expanding the left-hand side about x as $\varepsilon R \to 0^+$, we have

$$\mu_0^\mathbf{n} + \varepsilon(\mu_1^\mathbf{n} + R\partial_\mathbf{n}\mu_0^\mathbf{n}) + \varepsilon^2(\mu_2^\mathbf{n} + R\partial_\mathbf{n}\mu_1^\mathbf{n} + \frac{1}{2}R^2\partial_\mathbf{n}^2\mu_0^\mathbf{n}) + \dots, \tag{2.39}$$

10

and equating orders of ε the matching condition (2.38) yields

$$\mu_0^{\mathbf{n}} = \lim_{R \to \infty} \tilde{\mu}_0(s, R, \theta, t), \tag{2.40}$$

$$\mu_1^{\mathbf{n}} + R\partial_{\mathbf{n}}\mu_0^{\mathbf{n}} = \tilde{\mu}_1(s, R, \theta, t) + o(1) \qquad \text{as } R \to \infty, \tag{2.41}$$

$$\mu_2^{\mathbf{n}} + R\partial_{\mathbf{n}}\mu_1^{\mathbf{n}} + \frac{1}{2}R^2\partial_{\mathbf{n}}^2\mu_0^{\mathbf{n}} = \tilde{\mu}_2(s, R, \theta, t) + o(1) \qquad \text{as } R \to \infty, \tag{2.42}$$

$$\mu_3^{\mathbf{n}} + R\partial_{\mathbf{n}}\mu_2^{\mathbf{n}} + \frac{R^2\partial_{\mathbf{n}}^2\mu_1^{\mathbf{n}}}{2} + \frac{R^3\partial_{\mathbf{n}}^3\mu_0^{\mathbf{n}}}{6} = \tilde{\mu}_3(s, R, \theta, t) + o(1) \qquad \text{as } R \to \infty. \tag{2.43}$$

Similarly we obtain the matching conditions for u,

$$u_0^{\mathbf{n}} = \lim_{R \to \infty} \tilde{u}_0(s, R, \theta, t), \tag{2.44}$$

$$u_1^{\mathbf{n}} + R\partial_{\mathbf{n}}u_0^{\mathbf{n}} = \tilde{u}_1(s, R, \theta, t) + o(1) \qquad \text{as } R \to \infty, \tag{2.45}$$

$$u_2^{\mathbf{n}} + R\partial_{\mathbf{n}}u_1^{\mathbf{n}} + \frac{1}{2}R^2\partial_{\mathbf{n}}^2 u_0^{\mathbf{n}} = \tilde{u}_2(s, R, \theta, t) + o(1) \qquad \text{as } R \to \infty. \tag{2.46}$$

3. Fast Equilibration to the pore profile . In this section we consider the relaxation of an initial data an equilbria solution on the fast $T_j = t/\varepsilon^j$ time scales for $j = 2, 1$.

3.1. Time scale $T_2 = t/\varepsilon^2$: outer expansion. Far from the pore Γ, the solution and chemical potential admit the outer expansion

$$u(x, t) = u_0 + \varepsilon u_1 + \varepsilon^2 u_2 + \varepsilon^3 u_3 + \dots, \tag{3.1}$$

$$\mu(x, t) = \mu_0 + \varepsilon\mu_1 + \varepsilon^2\mu_2 + \dots, \tag{3.2}$$

where

$$u_i = u_i(x, T_2), \quad \mu_i = \mu_i(x, T_2), \quad T_2 = t/\varepsilon^2. \tag{3.3}$$

Substituting the expansion of u into the definition, (1.8), of μ we determine

$$\mu_0 = W''(u_0)W'(u_0) = G'(u_0), \tag{3.4}$$

$$\mu_1 = \left(W'''(u_0)W'(u_0) + W''(u_0)^2 \right) u_1 = G''(u_0)u_1, \tag{3.5}$$

where $G(u) := \frac{1}{2}(W'(u))^2$. Expanding the left- and right-hand sides of (1.8) yields the expressions

$$\partial_{T_2}u_0 = 0, \quad \partial_{T_2}u_1 = 0, \tag{3.6}$$

$$\partial_{T_2}u_2 = \Delta G'(u_0). \tag{3.7}$$

On the T_2 time scale, the solution u is stationary to first and second order.

3.2. Time scale $T_2 = t/\varepsilon^2$: inner expansion. We assume an inner expansion for u and μ of the form (2.28). Since $(s, z) = (s(x, T_2), z(x, T_2))$ the time derivative of u takes the form

$$u_t = \varepsilon^{-2}\left(\tilde{u}_{T_2} + \tilde{u}_s \frac{\partial s}{\partial T_2} + \nabla_z\tilde{u} \cdot \frac{\partial z}{\partial T_2} \right).$$

In light of the normal velocity relations (2.20)-(2.21) we obtain

$$u_t = -\varepsilon^{-3}\mathbf{V}_{-2} \cdot \nabla_z\tilde{u}_0 + \varepsilon^{-2}\Big(\frac{\partial\tilde{u}_0}{\partial T_2} + \frac{\partial\tilde{u}_0}{\partial s}\frac{\partial s}{\partial T_2} + \frac{\partial\tilde{u}_0}{\partial z_1}z_2\mathbf{N}^2 \cdot \frac{\partial\mathbf{N}^1}{\partial T_2}$$

$$+ \frac{\partial\tilde{u}_0}{\partial z_2}z_1\mathbf{N}^1 \cdot \frac{\partial\mathbf{N}^2}{\partial T_2} - \mathbf{V}_{-2} \cdot \nabla_z\tilde{u}_1 \Big) + O(\varepsilon^{-1}), \tag{3.8}$$

11

where $\mathbf{V}_{-2}$ denotes the normal velocity on the T_2 time scale. Matching the ε^{-3} and the ε^{-2} terms in (3.8) with the corresponding terms in the inner Laplacian expansion, (2.29), for the chemical potential μ we find

$$\mathbf{V}_{-2} \cdot \nabla_z \tilde{u}_0 = 0,$$

$$\frac{\partial \tilde{u}_0}{\partial T_2} + \frac{\partial \tilde{u}_0}{\partial s} \frac{\partial s}{\partial T_2} + \frac{\partial \tilde{u}_0}{\partial z_1} z_2 \mathbf{N}^2 \cdot \frac{\partial \mathbf{N}^1}{\partial T_2} + \frac{\partial \tilde{u}_0}{\partial z_2} z_1 \mathbf{N}^1 \cdot \frac{\partial \mathbf{N}^2}{\partial T_2} - \mathbf{V}_{-2} \cdot \nabla_z \tilde{u}_1 = \Delta_z \tilde{\mu}_0,$$

where $\tilde{\mu}_0$ is given by (2.31). We are interested in solutions based upon a quasi-stationary radial profile, consequently we assume that the transient dynamics on the T_2 have equilibrated, that is $\mathbf{V}_{-2} = 0$ and all T_2 partials are zero, so that the system of equations reduces to $\Delta_z \tilde{\mu}_0 = 0$. These assumptions are consistent with equilbria which at leading order have radially symmetric profiles that render $\tilde{\mu}_0 = 0$. Calculations for the T_1 time scale are similar, and are omitted. We deduce that

PROPOSITION 3.1. *Let U denote the nontrivial, radially-symmetric solution of*

$$-\Delta_z U + W'(U) = -\frac{\partial^2 U}{\partial R^2} - \frac{1}{R}\frac{\partial U}{\partial R} - \frac{1}{R^2}\frac{\partial^2 U}{\partial \theta^2} + W'(U) = 0 \qquad (3.9)$$

subject to the boundary condition $U \to b_- := -1$ exponentially as $|z| \to \infty$. Then the extension of U off of Γ_ℓ is an equilibrium of (1.8) on the T_2 and T_1 time-scales.

REMARK 3.2. *Equation (3.9) has many solutions, we denote the radially symmetric pore profile U_p from (1.6) by U, dropping the subscript p to simplify notation.*

A key role is played by the linearization

$$\mathcal{L} := -\Delta_z + W''(U), \qquad (3.10)$$

of (3.9) about U. This operator is self-adjoint in the R-weighted inner product, has strictly positive essential spectrum $[W''(b_-), \infty)$ and at least one negative eigenvalue. Moreover the translational eigenfunctions $\partial_{z_1} U$ and $\partial_{z_2} U$ lie in the kernel of $\mathcal{L}$. For each $m \in \mathbb{N}$ the spaces

$$\mathcal{Z}_m := \{ f(R)\cos(m\theta) + g(R)\sin(m\theta) \,\big|\, f, g \in C^\infty(0, \infty) \}.$$

are invariant under the operator $\mathcal{L}$, and mutually orthogonal in $L^2(\Omega)$. Moreover, on these spaces $\mathcal{L}$ reduces to

$$\mathcal{L}\big(f(R)\cos(m\theta) + g(R)(\sin m)\theta\big) = \cos(m\theta)\mathcal{L}_m f + \sin(m\theta)\mathcal{L}_m g,$$

where

$$\mathcal{L}_m := -\frac{\partial^2}{\partial R^2} - \frac{1}{R}\frac{\partial}{\partial R} + \frac{m^2}{R^2} + W''(U). \qquad (3.11)$$

Each operator $\mathcal{L}_m$ is self-adjoint on $\mathbb{R}_+$ in the R-weighted inner product, and moveover the operator $\mathcal{L}_1$ is non-negative with kernel spanned by $\partial_R U$. For $m > 1$ we deduce that each of $\mathcal{L}_m > \mathcal{L}_1$ is strictly positive. We address the kernel of $\mathcal{L}_0$ with the following assumption.

ASSUMPTION 3.3. *We assume that the operator $\mathcal{L}_0$ has no kernel, so that*

$$\ker(\mathcal{L}) = \mathrm{span}\{\partial_{z_1} U, \partial_{z_2} U\} = \mathrm{span}\{\partial_R U \cos\theta, \partial_R U \sin\theta\}. \qquad (3.12)$$

In particular the operator $\mathcal{L}_m$ is boundedly invertible for all $m \neq 1$.

We remark that any $f \in L^2(\mathbb{R}^2)$ admits the Fourier expansion

$$f = f_0(R) + \sum_{m=1}^{\infty} \left(f_m(R) \cos(m\theta) + g_m(R) \sin(m\theta) \right),$$

and so long as $\{f_1, g_1\} \perp \ker(\mathcal{L}_1)$, we have the inverse formulation

$$\mathcal{L}^{-1} f = \mathcal{L}_0^{-1} f_0 + \sum_{m=1}^{\infty} \left(\left(\mathcal{L}_m^{-1} f_m(R) \right) \cos(m\theta) + \left(\mathcal{L}_m^{-1} g_m(R) \right) \sin(m\theta) \right).$$

4. The time scale t =O(1). On the t time scale, we perform a regular expansion of the outer solution u and chemical potential μ as in (3.1) and (3.2). Matching the $O(1)$ terms in u_t and $\Delta\mu$, we obtain the nonlinear diffusion equation for u_0

$$\partial_t u_0 = \Delta \mu_0, \quad \mu_0 = G'(u_0), \tag{4.1}$$

which has stable equilibrium at the zeros of W', in particular $u_0 = b_-$ is a stable equilibrium.

4.1. Inner expansion. In the inner region, Γ_ℓ, we have an inner expansion, (2.28) of u and μ. As in (3.8) we expand the time derivative of u as

$$u_t = \tilde{u}_t + \tilde{u}_s \frac{\partial s}{\partial t} + \frac{\partial z}{\partial t} \cdot \nabla_z \tilde{u} = -\varepsilon^{-1} \mathbf{V}_0 \cdot \nabla_z \tilde{u}_0 + O(1), \tag{4.2}$$

where $\mathbf{V}_0$ denotes the normal velocity on the t time scale. Matching (4.2) and (2.29), the ε^{-2} and ε^{-1} terms give

$$0 = \Delta_z \tilde{\mu}_0, \tag{4.3}$$
$$-\mathbf{V}_0 \cdot \nabla_z \tilde{u}_0 = \Delta_z \tilde{\mu}_1 - \vec{\kappa} \cdot \nabla_z \tilde{\mu}_0. \tag{4.4}$$

Equation (4.3) is consistent with the leading order solution $u(x,t) = U(z)$, which renders $\tilde{\mu}_0 = 0$. Consequently, (4.4) simplifies to

$$\mathbf{V}_0 \cdot \nabla_z U = -\Delta_z \tilde{\mu}_1. \tag{4.5}$$

To determine $\mathbf{V}_0$ we must determine an explicit solution for $\tilde{\mu}_1$ in (4.5), subject to matching conditions with the outer solution. Turning to polar coordinates, $z_1 = R\cos\theta$, $z_2 = R\sin\theta$, we write $\tilde{\mu}_1$ in its Fourier series

$$\tilde{\mu}_1 = A(s,R)\cos\theta + B(s,R)\sin\theta + C(s,R) + \xi(s,R,\theta), \tag{4.6}$$

where

$$\xi(s,R,\theta) = \sum_{m=2}^{\infty} \left(A_m(s,R) \cos m\theta + B_m(s,R) \sin m\theta \right). \tag{4.7}$$

The Cartesian Laplacian in z transforms to the familiar polar Laplacian in R and θ, while the left-hand side of (4.5) transforms to

$$\mathbf{V}_0 \cdot \nabla_z U = U'(R) \left(V_{01} \cos\theta + V_{02} \sin\theta \right). \tag{4.8}$$

13

Substituting these expansions into (4.5) and matching terms yields the system

$$\frac{\partial^2 A}{\partial R^2} + \frac{1}{R}\frac{\partial A}{\partial R} - \frac{1}{R^2}A = -V_{01}U'(R), \tag{4.9}$$

$$\frac{\partial^2 B}{\partial R^2} + \frac{1}{R}\frac{\partial B}{\partial R} - \frac{1}{R^2}B = -V_{02}U'(R), \tag{4.10}$$

$$\frac{\partial^2 C}{\partial R^2} + \frac{1}{R}\frac{\partial C}{\partial R} = 0, \tag{4.11}$$

$$\frac{\partial^2 A_m}{\partial R^2} + \frac{1}{R}\frac{\partial A_m}{\partial R} - \frac{m^2}{R^2}A_m = 0, \quad m = 2, 3, \ldots. \tag{4.12}$$

$$\frac{\partial^2 B_m}{\partial R^2} + \frac{1}{R}\frac{\partial B_m}{\partial R} - \frac{m^2}{R^2}B_m = 0, \quad m = 2, 3, \ldots. \tag{4.13}$$

Excluding singularities, the solutions to (4.12) and (4.13) take the form

$$A_m(s, R) = a_m(s)R^m, \quad B_m(s, R) = b_m(s)R^m, \quad m = 2, 3, \ldots, \tag{4.14}$$

while (4.11) yields $C = C_0(s)$, and (4.9) and (4.10) have solutions

$$A(s, R) = C_{01}(s)R - V_{01}(s)a(R), \quad B(s, R) = C_{02}R - V_{02}(s)a(R),$$

where a satisfies

$$a''(R) + \frac{1}{R}a'(R) - \frac{1}{R^2}a(R) = \frac{1}{R^2}\frac{d}{dR}\left(R^3\frac{d}{dR}\left(\frac{a}{R}\right)\right) = U'(R). \tag{4.15}$$

This equation has the inhomogeneous solution

$$a(R) = \frac{1}{R}\int_0^R r\hat{U}\, dr, \tag{4.16}$$

where we have introduced $\hat{U} := U - b_-$ which is positive and tends to zero exponentially as $R \to \infty$. The chemical potential $\tilde{\mu}_1$ takes the general form

$$\tilde{\mu}_1 = C_0(s) + (C_{01}(s)R - V_{01}(s)a(R))\cos\theta + (C_{02}R - V_{02}a(R))\sin\theta$$
$$+ \sum_{m=2}^{\infty}\left(a_m(s)R^m\cos m\theta + b_m(s)R^m\sin m\theta\right). \tag{4.17}$$

However, simplifying the relation (2.32) between $\tilde{\mu}_1$ and $\tilde{u}_1$, we find that

$$\tilde{\mu}_1 = \mathcal{L}^2\tilde{u}_1 \tag{4.18}$$

where we have introduced the linearization about U,

$$\mathcal{L} := -\Delta_z + W''(U). \tag{4.19}$$

In particular, $\tilde{\mu}_1$ is in the range of $\mathcal{L}$, and hence perpendicular to $\ker(\mathcal{L})$. From Assumption 3.3 this requires

$$\int_{\mathbb{R}^2}\tilde{\mu}_1\partial_{z_i}\hat{U}\, dz = 0, \tag{4.20}$$

14

for $i = 1, 2$. From orthogonality in θ, the only non-trivial condition is imposed on the $\sin \theta$ and $\cos \theta$ terms in $\tilde{\mu}_1$. For $i = 1, 2$, the condition (4.20) reduces to

$$0 = \int_0^\infty \left(C_{0i} R - V_{0i} a(R) \right) U'(R) R \, dR, \tag{4.21}$$

which after integration by parts yields the relation

$$C_{0i}(s) = \frac{S_2}{2S_1} V_{0i}(s), \tag{4.22}$$

where we have introduced

$$S_1 := \int_0^\infty \hat{U}(R) R \, dR > 0, \quad \text{and} \quad S_2 := \int_0^\infty \hat{U}^2(R) R \, dR > 0. \tag{4.23}$$

The normal velocity $\mathbf{V}$ is determined through matching conditions between the inner and the outer expansions. From (2.41) we see that $\tilde{\mu}_1$ grows at most linearly as $R \to \infty$ and

$$\lim_{R \to \infty} \frac{\partial \tilde{\mu}_1}{\partial R}(s, R, \theta, t) = \partial_{\mathbf{n}} \mu_0^{\mathbf{n}} = \cos \theta \, \mathbf{N}^1 \cdot \nabla_x \mu_0^{\mathbf{n}} + \sin \theta \, \mathbf{N}^2 \cdot \nabla_x \mu_0^{\mathbf{n}}. \tag{4.24}$$

Comparing these conditions with (4.17), we deduce that $a_m = b_m = 0$, $m \geq 2$. Moreover, since

$$\frac{\partial \tilde{\mu}_1}{\partial R}(s, R, \pi + \theta, t) = -\frac{\partial \tilde{\mu}_1}{\partial R}(s, R, \theta, t), \tag{4.25}$$

we deduce from (4.24) that the $\partial_{\mathbf{n}} \mu_0^{\mathbf{n}}$ satisfies the jump condition, see (2.37),

$$[\partial_{\mathbf{n}} \mu_0^{\mathbf{n}}]_\Gamma = 0, \tag{4.26}$$

for any choice of normal vector $\mathbf{n}$. We simplify the left-hand side of (4.24)

$$\frac{\partial \tilde{\mu}_1}{\partial R}(s, R, \theta, t) = V_{01} \left(\frac{S_2}{2S_1} - \frac{\partial a}{\partial R} \right) \cos \theta + V_{02} \left(\frac{S_2}{2S_1} - \frac{\partial a}{\partial R} \right) \sin \theta. \tag{4.27}$$

and equating coefficients of $\sin \theta$ and $\cos \theta$ in (4.24) yields

$$\mathbf{N}^i \cdot \nabla_x \mu_0^{\mathbf{N}^i} = V_{0i} \left(\frac{S_2}{2S_1} - \lim_{R \to \infty} \frac{\partial a}{\partial R} \right), \tag{4.28}$$

and since a decays as $R \to \infty$ we find that

$$V_{0i} = \frac{2S_1}{S_2} \mathbf{N}^i \cdot \nabla_x \mu_0^{\mathbf{N}^i}, \tag{4.29}$$

for $i = 1, 2$. Combining equations (4.1), (4.26), and (4.29), yields the sharp interface limit problem for the evolution of Γ,

$$\partial_t u_0 = \Delta \mu_0 \qquad \text{in } \Omega \setminus \Gamma(t), \tag{4.30}$$
$$\mathbf{n} \cdot \nabla_x u_0 = 0 \qquad \text{on } \partial\Omega, \tag{4.31}$$
$$u_0 = b_- \qquad \text{on } \Gamma, \tag{4.32}$$
$$[\partial_{\mathbf{n}} \mu_0^{\mathbf{n}}]_\Gamma = 0 \qquad \text{on } \Gamma, \text{ for all normal vectors } \mathbf{n} \text{ of } \Gamma, \tag{4.33}$$

$$V_{0i} = \frac{2S_1}{S_2} \mathbf{N}^i \cdot \nabla_x \mu_0^{\mathbf{N}^i} \quad \text{for all } x \in \Gamma(t), i = 1, 2, \tag{4.34}$$

where the chemical potential $\mu_0 = W''(u_0)W'(u_0)$. The analysis of the transient solutions of (4.30)–(4.34) is beyond the scope of this paper, however the equilibria are trivial.

LEMMA 4.1. *Assume that the co-dimension two interface $\Gamma \subset (\Omega)$ has finite one dimensional Hausdorff measure. Then the only equilibrium solution of (4.30)-(4.34) is the trivial solution $u_0(x,t) \equiv b_-$, however the curve Γ can have arbitrary shape.*

Proof. At equilibrium we have $\Delta \mu_0 = 0$ in $\Omega \backslash \Gamma$ subject to $\mathbf{n} \cdot \nabla_x \mu_0 = 0$ and $\mu_0 = 0$ on Γ. From classic regularity theory it follows that $\mu_0 \in \mathcal{C}^2(\Omega \backslash \Gamma)$ and is bounded over all of Ω. Since the one dimensional Hausdorff measure of Γ is finite, it has zero one dimensional capacity and hence μ_0 is harmonic on all of Ω, see [26] or the example on page 29 of [12]. By the strong maximum principle if follows that μ_0, and hence u_0 are constant. Since $u_0 = b_-$ on Γ, we deduce that $u_0 \equiv b_-$. $\square$

We subsequently assume the system has achieved equilibrium on the t time-scale.

5. The time scale $t_1 = \varepsilon t$: Quenched mean-curvature flow. On the slow time-scale, $t_1 = \varepsilon t$, we use a matched inner-outer asymptotic expansion to derive a curvature driven flow for the normal velocity of the close-loop pore structures. However the normal velocity is quenched by the leading order outer chemical potential, $\mu_1 = \mu_1(t_1)$ which is driven to zero at an exponential rate.

5.1. Outer expansion. On the outer scale, matching the terms in u_t and $\Delta \mu$ in (1.8), we obtain

$$0 = \Delta \mu_0, \quad \mu_0 = W''(u_0)W'(u_0), \tag{5.1}$$
$$\partial_{t_1} u_0 = \Delta \mu_1. \tag{5.2}$$

By assumption the system (4.30)–(4.32) has reached the equilibrium $u_0 = b_-$ in $\Omega \setminus \Gamma(t)$. In this case $\mu_0 = W''(b_-)W'(b_-) = 0$ and

$$\mu_1 = \left(W'''(u_0)W'(u_0) + W''(u_0)^2 \right) u_1 = \alpha_-^2 u_1, \tag{5.3}$$

so that (5.2) reduces to

$$\Delta u_1 = 0 \tag{5.4}$$

in $\Omega \setminus \Gamma(t)$.

5.2. Inner expansion. Forming an inner expansion, (2.28) for u and μ, the time derivative of u admits the expansion

$$u_t = \varepsilon \left(\tilde{u}_{t_1} + \frac{\partial \tilde{u}}{\partial s} \frac{\partial s}{\partial t_1} \right) + \varepsilon \frac{\partial z}{\partial t_1} \cdot \nabla_z \tilde{u} = -\mathbf{V}_1 \cdot \nabla_z \tilde{u}_0 + O(\varepsilon), \tag{5.5}$$

where we have introduced the normal velocity $\mathbf{V}_1 = (V_{11}, V_{12})^t$, on the t_1 time scale. Matching the ε^{-2}, ε^{-1} and ε^0 terms in (5.5) and (2.29) yields

$$0 = \Delta_z \tilde{\mu}_0, \tag{5.6}$$
$$0 = \Delta_z \tilde{\mu}_1 - \vec{\kappa} \cdot \nabla_z \tilde{\mu}_0, \tag{5.7}$$
$$-\mathbf{V}_1 \cdot \nabla_z \tilde{u}_0 = \Delta_z \tilde{\mu}_2 - \vec{\kappa} \cdot \nabla_z \tilde{\mu}_1 + \Delta_0 \tilde{\mu}_0. \tag{5.8}$$

16

The matching condition (2.40) and (5.6) imply that $\tilde{\mu}_0 = 0$ and hence $\tilde{u}_0 = U$ and (5.7) simplifies to

$$\Delta_z \tilde{\mu}_1 = 0. \tag{5.9}$$

This equation has solutions of the form

$$\tilde{\mu}_1 = C(s) + \sum_{m=1}^{\infty} \left(a_m(s) R^m \cos m\theta + b_m(s) R^m \sin m\theta \right). \tag{5.10}$$

Since $\mu_0 = 0$, the matching condition (2.41) implies that $a_m = b_m = 0$ for all $m \geq 1$ and hence $\tilde{\mu}_1 = \tilde{\mu}_1(s,t)$ is independent of z. Since $\tilde{u}_0 = U$, (2.32) reduces to

$$\tilde{\mu}_1 = \mathcal{L}(\mathcal{L}\tilde{u}_1 + \vec{\kappa} \cdot \nabla_z U) = \mathcal{L}^2 \tilde{u}_1. \tag{5.11}$$

To invert $\mathcal{L}^2$ we introduce the following functions.

LEMMA 5.1. *For $j = 1, 2$ there exist radially symmetric functions Φ_j which converge exponentially to asymptotic values α_-^{-j} as $R \to \infty$ such that $\Phi_j - \alpha_-^{-j} \in \ker(\mathcal{L})^\perp$ and which solve*

$$\mathcal{L}\Phi_1 = 1, \quad \text{and} \quad \mathcal{L}\Phi_2 = \Phi_1, \tag{5.12}$$

Proof. Since U converges to b_- at an exponential rate as $R \to \infty$, (5.12) is equivalent to

$$\mathcal{L}(\Phi_1 - \alpha_-^{-1}) = 1 - W''(U)/W''(b_-),$$

where the right-hand side lies in $\ker(\mathcal{L})^\perp \subset L^2$. Since the essential spectrum of $\mathcal{L}$ is bounded away from the origin, the operator is Fredholm of index zero and this problem has a unique solution which lies in $\ker(L)^\perp$. Since the right-hand side is radial, the solution is too. A similar argument holds for Φ_2. $\square$

Using Lemma 5.1 we solve (5.11) for $\tilde{u}_1$,

$$\tilde{u}_1 = \tilde{\mu}_1 \Phi_2(R), \tag{5.13}$$

and (5.8) simplifies to

$$\Delta_z \tilde{\mu}_2 = -\mathbf{V}_1 \cdot \nabla_z U. \tag{5.14}$$

As in Section 4, this equation has a solution of the form

$$\tilde{\mu}_2 = C_4(s) + (C_{11}(s)R - V_{11}a(R)) \cos \theta + (C_{12}(s)R - V_{12}a(R)) \sin \theta + \xi_2, \tag{5.15}$$

where a is defined in (4.16) and ξ_2 takes the form of the final term in (4.17). On the other hand, since $\tilde{u}_0 = U$ and $\tilde{u}_1$ satisfies (5.13), (2.33) simplifies to

$$\tilde{\mu}_2 = \mathcal{L}\left(\mathcal{L}\tilde{u}_2 + \vec{\kappa} \cdot \nabla_z \tilde{u}_1 - \Delta_0 U + \frac{1}{2} W'''(U) \tilde{u}_1^2 \right)$$
$$+ \left(\vec{\kappa} \cdot \nabla_z + W'''(U) \tilde{u}_1 \right) \left(\mathcal{L}\tilde{u}_1 + \vec{\kappa} \cdot \nabla_z U \right) + (\eta_1 - \eta_2) W'(U), \tag{5.16}$$

17

which can be rewritten as

$$\mathcal{L}\left(\mathcal{L}\tilde{u}_2 + \tilde{\mu}_1 \vec{\kappa} \cdot \nabla_z \Phi_2 + (z \cdot \vec{\kappa}) \vec{\kappa} \cdot \nabla_z U + \frac{1}{2} W'''(U) \tilde{\mu}_1^2 \Phi_2^2 \right) = \mathcal{R}_2, \tag{5.17}$$

where we have introduced

$$\mathcal{R}_2 := \tilde{\mu}_2 - (\vec{\kappa} \cdot \nabla_z)^2 U - \tilde{\mu}_1 (\vec{\kappa} \cdot \nabla_z \Phi_1 + W'''(U) \Phi_2 \vec{\kappa} \cdot \nabla_z U) - \tilde{\mu}_1^2 W'''(U) \Phi_1 \Phi_2$$
$$- (\eta_1 - \eta_2) W'(U).$$

In particular we may solve for $\tilde{u}_2$ if and only if $\mathcal{R}_2 \in \ker(\mathcal{L})^\perp$. Addressing these two conditions term by term we calculate that

$$\int_{\mathbb{R}^2} \tilde{\mu}_2 \frac{\partial U}{\partial z_i} \, dz = \pi \left(C_{1i} \int_0^\infty U'(r) r^2 \, dr - V_{1i} \int_0^\infty a(r) U'(r) r \, dr \right),$$
$$= -\pi \left(2 C_{1i} S_1 - V_{1i} S_2 \right), \tag{5.18}$$

where S_1 and S_2 were introduced in (4.23). The terms $(\kappa \cdot \nabla_z)^2 U \in (\mathcal{Z}_0 + \mathcal{Z}_2)$ and $W'''(U) \Phi_1 \Phi_2 \in \mathcal{Z}_0$ are orthogonal to $\partial_{z_i} U \in \mathcal{Z}_1$ while

$$(\mathcal{R}_2 - \tilde{\mu}_2, \partial_{z_i} U) = -\pi \tilde{\mu}_1 \kappa_i \int_0^\infty U' \left(\Phi_1' + W'''(U) \Phi_2 U' \right) R \, dR. \tag{5.19}$$

LEMMA 5.2. *The operator $\mathcal{L}$ satisfies*

$$\mathcal{L}\left(\frac{1}{2} R U'\right) = \frac{1}{2} \mathcal{L}_0(R U') = -\Delta_z U = -\left(U'' + \frac{1}{R} U'\right), \tag{5.20}$$

$$\mathcal{L}(\Delta_z U) = \mathcal{L}_0\left(U'' + \frac{1}{R} U'\right) = -W'''(U) |\nabla U|^2 = -W'''(U) U'^2. \tag{5.21}$$

Integrating by parts on the Φ_1' term in (5.19) and using (5.20)-(5.21) we obtain

$$(\mathcal{R}_2 - \tilde{\mu}_2, \partial_{z_i} U) = -\frac{\pi}{2} \tilde{\mu}_1 \kappa_i \int_0^\infty \left(\Phi_1 \mathcal{L}(R U') + \Phi_2 \mathcal{L}^2(R U') \right) R \, dR,$$
$$= -\pi \tilde{\mu}_1 \kappa_i \int_0^\infty R^2 U' dR = 2\pi \tilde{\mu}_1 \kappa_i S_1. \tag{5.22}$$

Combining (5.18) and (5.22) the solvability condition reduces to

$$\mathbf{C}_1(s) = \tilde{\mu}_1 \vec{\kappa} + \frac{S_2}{2 S_1} \mathbf{V}_1. \tag{5.23}$$

The normal velocity $\mathbf{V}_1$ is determined through the matching condition (2.42). Since $\mu_0 = 0$, this condition reduces to

$$\lim_{R \to \infty} \frac{\partial \tilde{\mu}_2}{\partial R}(s, R, \theta) = \partial_{\mathbf{n}} \mu_1^{\mathbf{n}}(s, \theta) = \mathbf{n} \cdot \nabla_x \mu_1^{\mathbf{n}}, \tag{5.24}$$

where $\mathbf{n} := \cos \theta \, \mathbf{N}^1 + \sin \theta \, \mathbf{N}^2$. As a consequence, $\xi_2 = 0$ in (5.15) and

$$\lim_{R \to \infty} \left((C_{11}(s) - V_{11} a'(R)) \cos \theta + (C_{12}(s) - V_{12} a'(R)) \sin \theta \right) = \mathbf{n} \cdot \nabla_x \mu_1^{\mathbf{n}}. \tag{5.25}$$

We deduce that $[\partial_{\mathbf{n}} \mu_1^{\mathbf{n}}]_\Gamma = 0$, moreover, $a'(R) \to 0$ as $R \to \infty$. Using (5.23) and equating coefficients of $\sin \theta$ and $\cos \theta$ we obtain

$$V_{1i} = \frac{2 S_1}{S_2} \left(\mathbf{N}^i \cdot \nabla_x \mu_1^{\mathbf{N}^i} - \tilde{\mu}_1(s) \kappa_i \right). \tag{5.26}$$

18

5.3. Sharp interface limit. On the t_1 time scale, the evolution of the interface, Γ, is given by the normal velocity

$$V_i = \frac{2S_1}{S_2}\left(\mathbf{N}^i \cdot \nabla_x \mu_1^{\mathbf{N}^i} - \mu_1 \kappa_i\right) \quad \text{on } \Gamma, \ i = 1, 2, \tag{5.27}$$

where μ_1 is the solution of the elliptic system

$$\Delta \mu_1 = 0 \qquad \text{in } \Omega \setminus \Gamma, \tag{5.28}$$
$$\mathbf{n} \cdot \nabla_x \mu_1 = 0 \qquad \text{on } \partial\Omega, \tag{5.29}$$
$$[\partial_{\mathbf{n}} \mu_1^{\mathbf{n}}]_\Gamma = 0 \qquad \text{on } \Gamma, \text{ for all normal vectors } \mathbf{n} \text{ of } \Gamma. \tag{5.30}$$

The inner chemical potential satisfies $\mu_1 = \tilde{\mu}_1(s, t_1)$ on Γ. However, the following Lemma shows that the solutions, μ_1 to this system are trivial.

LEMMA 5.3. *Suppose $\mu_1 \in C^2(\Omega \setminus \Gamma) \cap C(\bar{\Omega})$ satisfies (5.28) and (5.29) and Γ has finite one dimensional Hausdorff measure, then μ_1 is a spatial constant.*

Proof. By the arguments of Lemma 4.1 we deduce that $\Delta \mu_1 = 0$ on all of Ω. The result then follows from the strong maximum principle. $\square$

It remains to determine the spatially constant value $\mu_1 = \mu_1(t_1)$, which is determined by mass conservation. Since $\nabla_x \mu_1 = 0$ the normal velocity reduces to

$$\mathbf{V} = -\frac{2S_1}{S_2}\mu_1 \vec{\kappa}. \tag{5.31}$$

Denoting the total mass of the minority phase by M_0, we decompose it as

$$M_0 = \int_{\Omega \setminus \Gamma_\ell} (u - b_-) \, dx + \int_{\Gamma_\ell} (u - b_-) dx. \tag{5.32}$$

Solving (5.3) for μ_1 the outer integral becomes

$$\int_{\Omega \setminus \Gamma_\ell} (u - b_-) \, dx = \int_{\Omega \setminus \Gamma_\ell} \varepsilon \alpha_-^{-2} \mu_1 \, dx + O(\varepsilon^2), \tag{5.33}$$
$$= \varepsilon \alpha_-^{-2} \mu_1 (|\Omega| - |\Gamma_\ell|) + O(\varepsilon^2),$$

while absorbing the $|\Gamma_\ell|$ term in (5.33) into the inner integral, changing variables, and recalling (2.22) yields

$$\int_{\Gamma_\ell} (\tilde{u} - b_-) - \varepsilon \alpha_-^{-2} \mu_1 \, dx = \int_\Gamma \int_{\mathbb{R}^2} \left((\tilde{u} - b_-) - \varepsilon \alpha_-^{-2} \mu_1\right) J(s, z) \, ds \, dz.$$
$$= \int_\Gamma \int_{\mathbb{R}^2} \left(\hat{U} + \varepsilon(\tilde{u}_1 - \mu_1 \alpha_-^{-2})\right) (\varepsilon^2 - \varepsilon^3 z \cdot \vec{\kappa}) \, dz \, ds$$
$$= 2\pi |\Gamma| \left(S_1 \varepsilon^2 + \mu_1 S_3 \varepsilon^3\right) + O(\varepsilon^4 |\Gamma|), \tag{5.34}$$

where $\hat{U}$ is orthogonal to z and we introduced

$$S_3 := \int_0^\infty (\Phi_2 - \alpha_-^{-2}) \, R \, dR > 0. \tag{5.35}$$

Combining (5.34) and (5.33), we have

$$M_0 = \alpha_-^{-2} \mu_1 |\Omega| \varepsilon + 2\pi S_1 |\Gamma| \varepsilon^2 + 2\pi \mu_1 |\Gamma| S_3 \varepsilon^3 + O(\varepsilon^4 |\Gamma|). \tag{5.36}$$

We consider this balance under various configurations.

5.3.1. $|\Gamma|$ **is** $O(\varepsilon^{-1})$**.** We expand the length of Γ as

$$|\Gamma| = \varepsilon^{-1}\gamma_{-1} + \gamma_0 + \varepsilon\gamma_1 + O(\varepsilon^2), \tag{5.37}$$

and writing $M_0 = \varepsilon\tilde{M}_0 + \varepsilon^2\tilde{M}_1 + O(\varepsilon^2)$, (5.36) yields

$$\tilde{M}_0 = \alpha_-^{-2}|\Omega|\mu_1 + 2\pi S_1\gamma_{-1}. \tag{5.38}$$

Taking the t_1 derivative of this expression we determine that

$$\frac{d|\Gamma|}{dt_1} = \varepsilon^{-1}\frac{d\gamma_{-1}}{dt_1} + O(1) = -\varepsilon^{-1}\frac{|\Omega|}{2\pi\alpha_-^2 S_1}\frac{d\mu_1}{dt_1} + O(1). \tag{5.39}$$

On the other hand,

$$\frac{d|\Gamma|}{dt_1} = -\int_\Gamma \mathbf{V} \cdot \vec{\kappa} \, ds = \frac{2S_1}{S_2}\mu_1\int_\Gamma |\vec{\kappa}|^2 \, ds. \tag{5.40}$$

Equating the two expressions yields the leading order evolution equation

$$\frac{d\mu_1}{dt_1} = -\varepsilon\frac{4\pi\alpha_-^2 S_1^2}{|\Omega|S_2}\mu_1\int_\Gamma |\vec{\kappa}|^2 \, ds. \tag{5.41}$$

From (4.23), $S_1, S_2 > 0$, and μ_1 decays exponentially to 0 on the t_1 time scale, while the normal velocity is driven by either a mean curvature flow for $\mu_1 < 0$, or a backwards mean curvature flow for $\mu_1 > 0$.

5.3.2. $|\Gamma|$ **is** $O(1)$**.** Since the total mass M_0 of the minority species is conserved, we see that $\mu_1'(t_1) = O(\varepsilon)$, and μ_1 is constant on this time-scale. If moreover, $M_0 = O(\varepsilon^2)$, then $\mu_1 = 0$ to leading order.

6. Length-Preserving Willmore flow on the slow time scale. Assuming a relaxation to equilibrium on the t_1 time-scale, we find that well-separated collections of closed-loop pores evolve according to a length-preserving Willmoresque flow on the $t_2 = \varepsilon^2 t$ time-scale.

6.1. Outer expansion. On the slow time scale, $t_2 = \varepsilon^2 t$, from the result of Section 5, the outer expansion takes the from

$$u = u_0 + \varepsilon^2 u_2 + \varepsilon^3 u_3 + \dots, \tag{6.1}$$
$$\mu = \varepsilon^2\mu_2 + \varepsilon^3\mu_3 + \dots. \tag{6.2}$$

Since $u_0 = b_-$, we see that $\partial_t u = O(\varepsilon^4)$ and matching the terms in (1.8) we find

$$\Delta\mu_2 = 0. \tag{6.3}$$

6.2. Inner expansion. Similarly, the inner expansion reduces to

$$u(x,t) = \tilde{u}(s,z,t) = \tilde{u}_0 + \varepsilon^2\tilde{u}_2 + \varepsilon^3\tilde{u}_3 + \dots, \tag{6.4}$$
$$\mu(x,t) = \tilde{\mu}(s,z,t) = \varepsilon^2\tilde{\mu}_2 + \varepsilon^3\tilde{\mu}_3 + \dots, \tag{6.5}$$

where $\tilde{u}_0 = U$ and the time derivative takes the form

$$u_t = \varepsilon^2\left(\tilde{u}_{t_2} + \frac{\partial\tilde{u}}{\partial s}\frac{\partial s}{\partial t_2}\right) + \varepsilon^2\frac{\partial z}{\partial t_2} \cdot \nabla_z\tilde{u} = -\varepsilon\mathbf{V}_2 \cdot \nabla_z\tilde{u}_0 + O(\varepsilon^2). \tag{6.6}$$

where $\mathbf{V}_2 = (V_{21}, V_{22})^t$ is the normal velocity on the t_2 time scale. Matching terms in (6.6) and (2.29), we arrive at

$$0 = \Delta_z \tilde{\mu}_2, \tag{6.7}$$

$$-\mathbf{V}_2 \cdot \nabla_z U = \Delta_z \tilde{\mu}_3 - \vec{\kappa} \cdot \nabla_z \tilde{\mu}_2. \tag{6.8}$$

As at the previous time scales, matching conditions imply that $\tilde{\mu}_2 = \tilde{\mu}_2(s)$ is constant in R and θ, depending only upon position along the curve Γ. Moreover the relation (2.33) reduces to

$$\tilde{\mu}_2 = \mathcal{L}^2 \tilde{u}_2 - (\vec{\kappa} \cdot \nabla_z)^2 U + (\eta_1 - \eta_2)\Delta_z U. \tag{6.9}$$

We solve this equation via the following Lemma.

LEMMA 6.1. *For $i, j = 1, 2$, there exist unique $\Phi_{ij} \in (\mathcal{Z}_0 + \mathcal{Z}_2) \perp \ker(\mathcal{L})$ such that*

$$\mathcal{L}^2 \Phi_{ij} = \frac{\partial^2 U}{\partial z_i \partial z_j}. \tag{6.10}$$

Moreover these functions take the from

$$\begin{aligned}
\Phi_{11} &= \Phi_3(R) + \Phi_4(R) \cos 2\theta, \\
\Phi_{12} &= \Phi_{21} = \Phi_4(R) \sin 2\theta, \\
\Phi_{22} &= \Phi_3(R) - \Phi_4(R) \cos 2\theta,
\end{aligned} \tag{6.11}$$

where Φ_3 and Φ_4 depend only upon R.

Proof. The existence follows from Assumption 3.3 since $\frac{\partial^2 U}{\partial z_i z_j} \perp \ker(\mathcal{L})$ for $i, j = 1, 2$. To derive the functional form (6.11) we calculate that

$$\begin{aligned}
U_{z_1 z_1} &= \frac{1}{2}\left(U'' + \frac{1}{R}U'\right) + \frac{1}{2}\left(U'' - \frac{1}{R}U'\right)\cos 2\theta, \\
&= -\frac{1}{4}\left(\mathcal{L}_0 + \cos 2\theta \, \mathcal{L}_2\right)(RU') \tag{6.12}
\end{aligned}$$

$$U_{z_1 z_2} = \frac{1}{2}\left(U'' - \frac{1}{R}U'\right)\sin 2\theta = -\frac{1}{4}\sin 2\theta \, \mathcal{L}_2(RU'), \tag{6.13}$$

$$\begin{aligned}
U_{z_2 z_2} &= \frac{1}{2}\left(U'' + \frac{1}{R}U'\right) - \frac{1}{2}\left(U'' - \frac{1}{R}U'\right)\cos 2\theta, \\
&= -\frac{1}{4}\left(\mathcal{L}_0 - \cos 2\theta \, \mathcal{L}_2\right)(RU'). \tag{6.14}
\end{aligned}$$

By Assumption 3.3 the operators $\mathcal{L}_m$ are boundedly invertible for $m \neq 1$. From (5.20) it follows that (6.11) holds with

$$\Phi_3 := \frac{1}{2}\mathcal{L}_0^{-2}\left(U'' + \frac{1}{R}U'\right) = -\frac{1}{4}\mathcal{L}_0^{-1}(RU'), \tag{6.15}$$

$$\Phi_4 := \frac{1}{2}\mathcal{L}_2^{-2}\left(U'' - \frac{1}{R}U'\right) = -\frac{1}{4}\mathcal{L}_2^{-1}(RU'). \tag{6.16}$$

□

Using Lemmas 5.1 and 6.1 we solve (6.9) for $\tilde{u}_2$ in the form

$$\tilde{u}_2 = \tilde{\mu}_2 \Phi_2 + \sum_{i,j} \kappa_i \kappa_j \Phi_{ij} - (\eta_1 - \eta_2)(\Phi_{11} + \Phi_{22}), \tag{6.17}$$

$$= \tilde{\mu}_2 \Phi_2 + \left(|\vec{\kappa}|^2 - 2(\eta_1 - \eta_2) \right) \Phi_3 + \left((\kappa_1^2 - \kappa_2^2) \cos 2\theta + 2\kappa_1 \kappa_2 \sin 2\theta \right) \Phi_4.$$

Since $\tilde{\mu}_2$ is independent of z, (6.8) simplifies to

$$\Delta_z \tilde{\mu}_3 = -\mathbf{V}_2 \cdot \nabla_z U \tag{6.18}$$

As in Sections 4 and 5, the matching conditions yield a solution of the form

$$\tilde{\mu}_3 = C_3(s) + (C_{21}(s)R - V_{21}a(R)) \cos \theta + (C_{22}(s)R - V_{22}a(R)) \sin \theta, \tag{6.19}$$

where the functions C_3 and $\mathbf{C}_2 := (C_{21}, C_{22})^t$ are to be determined. Returning to (2.30), using $\tilde{u}_0 = U$ and $\tilde{u}_1 = 0$, and recalling the definition (2.26) of Δ_0, we derive the expression

$$\mathcal{R}_3 = \mathcal{L} \left(\mathcal{L}\tilde{u}_3 + \vec{\kappa} \cdot \nabla_z \tilde{u}_2 - \Delta_1 \tilde{u}_0 \right), \tag{6.20}$$

where he have introduced

$$\mathcal{R}_3 := \tilde{\mu}_3 - \vec{\kappa} \cdot \nabla_z \left(\mathcal{L}\tilde{u}_2 + (z \cdot \vec{\kappa})\vec{\kappa} \cdot \nabla_z U \right)$$

$$- \left((z \cdot \vec{\kappa})\vec{\kappa} \cdot \nabla_z + W'''(U)\tilde{u}_2 - (\partial_s^2 + \eta_1) \right) (\vec{\kappa} \cdot \nabla_z U). \tag{6.21}$$

We may solve for $\tilde{u}_3$ if and only if $\mathcal{R}_3 \in \ker(\mathcal{L})^\perp$. We address each term in this solvability condition in turn. As in (5.18) we have

$$\int_{\mathbb{R}^2} \tilde{\mu}_3 U_{z_i} \, dz = -\pi (2C_{2i}S_1 - V_{2i}S_2) \tag{6.22}$$

Using (6.12)-(6.14) and (6.17) on the $\mathcal{L}\tilde{u}_2$ term yields

$$(\vec{\kappa} \cdot \nabla_z(\mathcal{L}\tilde{u}_2), U_{z_1})_{L^2} = - (\mathcal{L}\tilde{u}_2, \kappa_1 U_{z_1 z_1} + \kappa_2 U_{z_1 z_2})_{L^2},$$

$$= \frac{1}{4} (\mathcal{L}\tilde{u}_2, \kappa_1 \mathcal{L}_0(RU') + (\kappa_1 \cos 2\theta + \kappa_2 \sin 2\theta)\mathcal{L}_2(RU'))_{L^2},$$

$$= \frac{1}{4} \left(\tilde{\mu}_2 + (\frac{1}{2}|\vec{\kappa}|^2 - \eta_1 + \eta_2)\frac{1}{R}(RU')', \kappa_1 RU' \right)_{L^2}$$

$$+ \frac{1}{8} \left((\kappa_1^2 - \kappa_2^2)\kappa_1 \cos^2 2\theta + 2\kappa_1^2 \kappa_2 \sin^2 2\theta)(U'' - \frac{1}{R}U'), RU' \right)_{L^2}.$$

Switching to polar coordinates and carrying out the θ integration we obtain

$$(\vec{\kappa} \cdot \nabla_z(\mathcal{L}\tilde{u}_2), U_{z_i})_{L^2} = \frac{\pi}{2} \int_0^\infty \kappa_i \tilde{\mu}_2 R^2 U' + (\frac{1}{2}|\vec{\kappa}|^2 - \eta_1 + \eta_2)\kappa_i(RU')'RU' \, dR$$

$$+ \frac{\pi}{8}|\vec{\kappa}|^2 \kappa_i \int_0^\infty (U'' - \frac{1}{R}U')R^2 U' \, dR,$$

$$= -\pi \left(\tilde{\mu}_2 S_1 + \frac{|\vec{\kappa}|^2}{4} S_4 \right) \kappa_i, \tag{6.23}$$

for $i = 1, 2$, where we have introduced

$$S_4 := \int_0^\infty (U')^2 R \, dR > 0. \tag{6.24}$$

For the other $\tilde{u}_2$ term, using (5.20) and (5.21) we find

$$(W'''(U)\tilde{u}_2\vec{\kappa}\cdot\nabla_z U, U_{z_1})_{L^2} = \frac{1}{2}\int_{\mathbb{R}^2} \tilde{u}_2(\kappa_1\cos^2\theta + \kappa_2\cos\theta\sin\theta)\mathcal{L}_0^2(RU')\,dz.$$

Substituting (6.17) for $\tilde{u}_2$, the θ-integrals are zero, except for the product of the $\cos^2\theta$ term and the θ-independent terms of $\tilde{u}_2$. For $i = 1, 2$ these terms yield

$$\begin{aligned}(W'''(U)\tilde{u}_2\vec{\kappa}\cdot\nabla_z U, U_{z_i})_{L^2} &= \frac{\pi}{2}\kappa_i\int_0^\infty (\tilde{\mu}_2\Phi_2 + (|\vec{\kappa}|^2 - 2\eta_1 + 2\eta_2)\Phi_3)\mathcal{L}_0^2(RU')R\,dR \\ &= \frac{\pi}{2}\kappa_i\int_0^\infty \left(\tilde{\mu}_2 + (\frac{1}{2}|\vec{\kappa}|^2 - \eta_1 + \eta_2)\frac{1}{R}(RU')'\right)(RU')R\,dR \\ &= -\pi S_1\tilde{\mu}_2\kappa_i.\end{aligned} \tag{6.25}$$

There are two terms involving only curvature-gradients of U, the first satisfies

$$\begin{aligned}(\vec{\kappa}\cdot\nabla_z((z\cdot\vec{\kappa})\vec{\kappa}\cdot\nabla_z U), U_{z_i})_2 &= -\left((z\cdot\vec{\kappa})\vec{\kappa}\cdot\nabla_z U, (\vec{\kappa}\cdot\nabla_z U)_{z_i}\right)_2, \\ &= \frac{1}{2}\kappa_i\int_{\mathbb{R}^2} |\vec{\kappa}\cdot\nabla_z U|^2\,dz = \frac{\pi}{2}\kappa_i|\vec{\kappa}|^2\int_0^\infty (U')^2 R\,dR = \frac{\pi}{2}S_4\kappa_i|\vec{\kappa}|^2.\end{aligned} \tag{6.26}$$

Integrating by parts on the second term of this type yields

$$((z\cdot\vec{\kappa})\vec{\kappa}\cdot\nabla_z(\vec{\kappa}\cdot\nabla_z U), U_{z_i})_{L^2} = -\left(\vec{\kappa}\cdot\nabla_z U, |\vec{\kappa}|^2 U_{z_i} + (z\cdot\vec{\kappa})(\vec{\kappa}\cdot\nabla_z U)_{z_i}\right)_{L^2},$$

where the second term on the right-hand side is evaluate as above. Expanding the first term on the right-hand side we obtain

$$((z\cdot\vec{\kappa})\vec{\kappa}\cdot\nabla_z(\vec{\kappa}\cdot\nabla_z U), U_{z_i})_{L^2} = -\frac{\pi}{2}S_4\kappa_i|\vec{\kappa}|^2. \tag{6.27}$$

For $i = 1, 2$, the surface diffusion terms in the solvability condition evaluate to

$$\left((\partial_s^2 + \eta_1)\vec{\kappa}\cdot\nabla_z U, U_{z_i}\right)_{L^2} = \pi S_4(\partial_s^2 + \eta_1)\kappa_i. \tag{6.28}$$

Combining (6.22)-(6.23) with (6.25)-(6.27), the solvability condition reduces to

$$2S_1\mathbf{C}_2 - S_2\mathbf{V} = S_4\left(\partial_s^2 + \eta_1 + \frac{2S_1}{S_4}\tilde{\mu}_2 + \frac{1}{4}|\vec{\kappa}|^2\right)\vec{\kappa} \tag{6.29}$$

where S_1 and S_2 are as defined in (4.23) and (6.24) respectively. Since $\mu_0 = \mu_1 = 0$, the matching condition (2.43) reduces to

$$\lim_{R\to\infty} \frac{\partial\tilde{\mu}_3}{\partial R}(s, R, \theta) = \partial_{\mathbf{n}}\mu_2^{\mathbf{n}} \tag{6.30}$$

for $\mathbf{n} = \cos\theta\,\mathbf{N}^1(s) + \sin\theta\,\mathbf{N}^2$. As in Sections 4 and 5, we deduce that

$$[\partial_{\mathbf{n}}\mu_2^{\mathbf{n}}]_\Gamma = 0, \tag{6.31}$$

$$C_{2i}(s) = \mathbf{N}^i\cdot\nabla_x\mu_2^{\mathbf{N}^i}, \tag{6.32}$$

for $i = 1, 2$, and solving (6.29) for the normal velocity yields

$$V_{2i} = \frac{2S_1}{S_2}\mathbf{N}^i\cdot\nabla_x\mu_2^{\mathbf{N}^i} - \frac{S_4}{S_2}\left(\partial_s^2 + \eta_1 + \frac{2S_1}{S_4}\tilde{\mu}_2 + \frac{3}{4}|\vec{\kappa}|^2\right)\kappa_i. \tag{6.33}$$

23

6.3. Sharp interface limit. Since the outer chemical potential solves $\Delta\mu_2 = 0$ on $\Omega\backslash\Gamma(t)$ subject to homogeneous Neumann conditions on $\partial\Omega$ and $[\partial_{\mathbf{n}}\mu_2^{\mathbf{n}}]_\Gamma = 0$, it follows from Lemma 5.3 that $\mu_2 = \mu_2(t_2)$ is a spatial constant. Consequently $\nabla_x\mu_2 = 0$ and the normal velocity reduces to

$$\mathbf{V}_2 = -\frac{S_4}{S_2}\left(\partial_s^2 + \eta_1 + \frac{2S_1}{S_4}\mu_2 + \frac{1}{4}|\vec{\kappa}|^2\right)\vec{\kappa}. \tag{6.34}$$

As in Section 5, the value of the chemical potential, μ_2, is determined through the conservation of the minority phase. Since $u_0 = b_-$ and $u_1 = 0$ in $\Omega \setminus \Gamma_\ell$, the outer chemical potential satisfies

$$\mu_2 = W''(u_0)^2 u_2 = \alpha_-^2 u_2, \tag{6.35}$$

and hence $u_2 = u_2(t_2)$ is a spatial constant. The mass of the minority phase satisfies

$$M_0 = \int_{\Omega\backslash\Gamma_\ell}(u - b_-)\,dx + \int_{\Gamma_\ell}(\tilde{u} - b_-)\,dx,$$
$$= \int_\Omega(u - b_-)\,dx + \int_{\Gamma_\ell}\tilde{u} - b_- - \varepsilon^2\alpha_-^{-2}\mu_2\,dx. \tag{6.36}$$

As in (5.34) we have

$$\int_\Omega(u - b_-)\,dx = \int_\Omega(\varepsilon^2 u_2 + O(\varepsilon^3))\,dx = \varepsilon^2\alpha_-^{-2}|\Omega|\mu_2 + O(\varepsilon^3). \tag{6.37}$$

For the inner integral, recalling (2.22) we have

$$\int_{\Gamma_\ell}(\tilde{u} - b_-) - \varepsilon^2\alpha_-^{-2}\mu_2\,dx = \int_\Gamma\int_{\mathbb{R}^2}\left((\tilde{u} - b_-) - \varepsilon^2\alpha_-^{-2}\mu_2\right)J(z,s)\,dz\,ds$$
$$= \int_\Gamma\int_{\mathbb{R}^2}(\hat{U} + \varepsilon^2(\tilde{u}_2 - \alpha_-^{-2}\mu_2))(\varepsilon^2 - \varepsilon^3 z\cdot\vec{\kappa})\,dz\,ds + O(\varepsilon^5|\Gamma|)$$
$$= \varepsilon^2 2\pi S_1|\Gamma| + \varepsilon^4 2\pi|\Gamma|(S_3\mu_2 + S_5|\kappa|^2) + O(\varepsilon^5|\Gamma|), \tag{6.38}$$

where the $O(\varepsilon^3)$ term is zero by parity, we used (6.17) to eliminate $\tilde{u}_2$, and introduced

$$S_5 := \int_0^\infty\Phi_3(R)R\,dR, \tag{6.39}$$

where Φ_3 is defined in (6.11), and has indefinite sign. Combining (6.37) and (6.38), the mass of the minority phase is expressed as

$$M_0 = \varepsilon^2\left(\alpha_-^{-2}|\Omega|\mu_2 + 2\pi S_1|\Gamma|\right) + \varepsilon^4|\Gamma|2\pi S_5\mu_2 + O(\varepsilon^5|\Gamma|). \tag{6.40}$$

6.3.1. Case I: $|\Gamma_0|$ is of order $O\left(\varepsilon^{-1}\right)$. In this case $M_0 = O(\varepsilon)$, and expanding $|\Gamma|$ and M_0 as

$$|\Gamma| = \varepsilon^{-1}\gamma_{-1} + \gamma_0 + \varepsilon\gamma_1 + O(\varepsilon^2), \quad M_0 = \varepsilon\tilde{M}_0 + \varepsilon^2\tilde{M}_1 + O(\varepsilon^3), \tag{6.41}$$

the mass balance (6.40) requires

$$\tilde{M}_0 = 2\pi S_1\gamma_{-1}, \quad \tilde{M}_1 = 2\pi S_1\gamma_0 + \alpha_-^{-2}|\Omega|\mu_2. \tag{6.42}$$

24

Since the mass M_0 is conserved, we deduce that $\gamma_{-1} = \tilde{M}_0/(2\pi S_1)$ is independent of time and hence $\partial_{t_2}|\Gamma| = O(\varepsilon)$.

By assumption, $\|\vec{\kappa}\|_{L^\infty(\Gamma)} = O(1)$ and from (6.34) we deduce that the normal velocity $\|\mathbf{V}_2\|_{L^\infty(\Gamma)} = O(1)$. Moreover, from (2.12) we have

$$\frac{d|\Gamma|}{dt_2} = -\int_\Gamma \vec{\kappa} \cdot \mathbf{V}_2 \, ds = O(\varepsilon), \tag{6.43}$$

and from (6.34), $\mu_2(t_2)$ must satisfy

$$\mu_2 = \frac{S_4}{2S_1} \frac{\int_\Gamma |\partial_s \vec{\kappa}|^2 - \eta_1 |\vec{\kappa}|^2 - \frac{1}{4}|\vec{\kappa}|^5 \, ds}{\int_\Gamma |\vec{\kappa}|^2 \, ds}. \tag{6.44}$$

This choice of μ_2 serves to preserve the length of Γ. Introducing the curvature-weighted projection associated to Γ, which acts on $\mathbf{F} = (f_1, f_2)^t \in L^2(\Gamma)$ as

$$\Pi_\Gamma[\mathbf{F}] := \mathbf{F} - \vec{\kappa} \frac{\int_\Gamma \mathbf{F} \cdot \vec{\kappa} \, ds}{\int_\Gamma |\vec{\kappa}|^2 \, ds},$$

then the normal velocity has the equivalent formulation

$$\mathbf{V}_2 = -\frac{S_4}{S_2} \Pi_\Gamma \left[\left(\partial_s^2 + \frac{1}{4}|\vec{\kappa}|^2 \right) \vec{\kappa} \right]. \tag{6.45}$$

where the constant η_1 drops out since $\Pi_\Gamma[\eta_1 \vec{\kappa}] = 0$.

6.3.2. Case II: $|\Gamma|$ is of order $O(1)$. In this case we expand $M_0 = \varepsilon^2 \tilde{M}_1 + O(\varepsilon^3)$ and $|\Gamma| = \gamma_0 + \varepsilon \gamma_1 + O(\varepsilon^2)$. The balance of terms in (6.40) yields

$$\tilde{M}_1 = 2\pi S_1 \gamma_0 + \alpha_-^{-2} |\Omega| \mu_2. \tag{6.46}$$

In particular, $\gamma_0 = \left(\tilde{M}_1 - \alpha_-^{-2} |\Omega| \mu_2 \right) / (2\pi S_1)$ and

$$\frac{d|\Gamma|}{dt_2} = -\frac{|\Omega| \mu_2'(t_2)}{2\pi S_1 \alpha_-^2} + O(\varepsilon). \tag{6.47}$$

From (6.34), the leading order terms yield the coupled system

$$\mu_2'(t_2) = 2\pi S_1 \alpha_-^2 |\Omega|^{-1} \int_\Gamma \mathbf{V} \cdot \vec{\kappa} \, ds, \tag{6.48}$$

$$\mathbf{V} = -\frac{S_4}{S_2} \left(\partial_s^2 + \eta_1 + \frac{2S_1}{S_4} \mu_2 + \frac{1}{4}|\vec{\kappa}|^2 \right) \vec{\kappa}. \tag{6.49}$$

7. Competitive Geometric Flows. In an amphiphilic system it is possible for bilayers and pore structures to co-exist on the slow time-scale, and compete with one-another for the surfactant phase. Indeed, consider the pore profile, $U = U_p$, constructed in (3.9) and the bilayer profile, U_b, which is the homoclinic solution of

$$\partial_r^2 U_b = W'(U_b), \tag{7.1}$$

subject to the condition $U_b \to b_-$ as $r \to \pm\infty$. We have shown that for any closed co-dimension two manifold, $\Gamma_p \subset \Omega \subset \mathbb{R}^3$, we may associate a pore solution of the form

$$u(x, t) = U_p(z_1, z_2) + \varepsilon^2 u_{2p}(x, t) + O(\varepsilon^3), \tag{7.2}$$

25

where $u_{2p}(x,t) \to \mu_2 \alpha_-^{-2}$ at an $O(1)$ exponential rate in the $\varepsilon-scaled$ distance, $|(z_1, z_2)|$, to Γ_p. Here $\mu_2 = \mu_2(t_2)$ is the spatially constant, time dependent value of the outer chemical potential. Similarly, in [8] we showed that for any co-dimension one hyper-surface, $\Gamma_b \subset \Omega \subset \mathbb{R}^3$, we may associate a bilayer solution of the form

$$u(x,t) = U_b(r) + \varepsilon^2 u_{2b}(x,t) + O(\varepsilon^3), \tag{7.3}$$

where U_b is the homoclinic solution of (7.1) and $u_{2b}(x,t) \to \mu_2 \alpha_-^{-2}$ at an $O(1)$ exponential rate in the $\varepsilon-scaled$ signed distance, r, to Γ_b. It is trivial to extend this construction to co-existing bilayer and pore structures, with a common value of the outer chemical potential μ_2, so long as the sub-manifolds are uniformly smooth and are an $O(1)$ distance from both self-intersection and intersection with each-other. Indeed the composite solution takes the form

$$u(x,t) = U_p(z_1, z_2) + U_b(r) + \varepsilon^2 \left(u_{2p}(x,t) + u_{2b}(x,t) - \frac{\mu_2}{\alpha_-^2} \right) + O(\varepsilon^3), \tag{7.4}$$

where the two morphologies, characterized by the disjoint co-dimension one and two manifolds Γ_b and Γ_p, compete with each-other for surfactant phase through the common, temporally varying, value of $\mu_2 = \mu_2(t_2)$.

The normal velocity of the bilayer and pore morphologies are given by (1.9) and (1.11), coupled through the outer chemical potential μ_2. The evolution of the outer chemical potential is determined by the mass constraint for the combined bilayer-pore structures. For u a combined bilayer-pore solution of the form (7.4), conservation of mass implies that

$$M := \int_\Omega (u_0 - b_-) \, dx = \int_\Omega (u(x,t) - b_-) \, dx$$
$$= \int_{\Gamma_{b,\ell}} \hat{U}_b(r(x)) \, dx + \int_{\Gamma_{p,\ell}} \hat{U}_p(z(x)) \, dx + O\left(\varepsilon^2 |\Gamma_p|, \varepsilon^2 |\Gamma_b| \right), \tag{7.5}$$

where $\Gamma_{b,\ell}$ and $\Gamma_{p,\ell}$ are the regions of Ω whose points are within $\varepsilon\ell$ of Γ_b and Γ_p respectively. A small total mass $M = \varepsilon M_0 + O(\varepsilon^2)$, requires that $|\Gamma_b| = O(1)$ and $|\Gamma_p| = O(\varepsilon^{-1})$. Changing to local variables in the mass constraint integrals yields the leading-order identity

$$m_b |\Gamma_b| + m_p \varepsilon |\Gamma_p| = M_0, \tag{7.6}$$

where m_b and m_p are introduced in (1.10) and Theorem 1.1. Equivalently, taking the time derivative we have

$$m_b \frac{d}{dt} |\Gamma_b| + m_p \varepsilon \frac{d}{dt} |\Gamma_p| = 0. \tag{7.7}$$

From (2.12), and the bilayer equivalent

$$\frac{d|\Gamma_b|}{dt} = \int_{\Gamma_b} V_b H \, dS,$$

the normal velocity expressions (1.9) and (1.11) yield leading-order expressions for change in bilayer surface area and pore length,

$$\frac{d|\Gamma_b|}{dt} = \frac{\sigma_b}{m_b} \int_{\Gamma_b} \left[\left(K - \frac{H^2}{2} + \frac{\eta_1 + \eta_2}{2} + \lambda_b \mu_2 \right) H^2 - |\nabla_s H|^2 \right] dS, \tag{7.8}$$
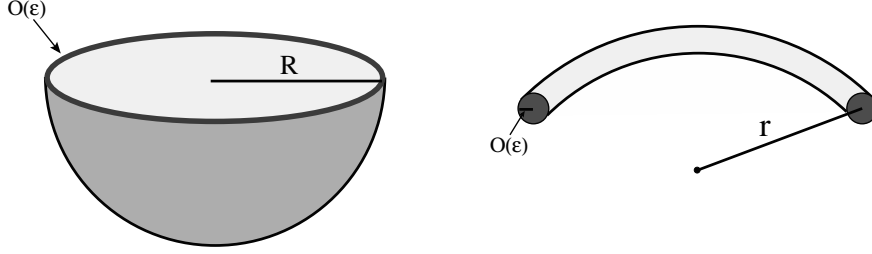
Figure 4: Bottom half of a spherical bilayer of radius R and an arc-length of a closed circular pore of radius $r > 0$. The structures are cut to show the inner width, which is $O(\varepsilon)$. The surfactant phase is colored blue, while the surface is yellow.

$$\frac{d|\Gamma_p|}{dt} = \frac{\sigma_p}{m_p} \int_{\Gamma_p} \left[\left(\frac{1}{4}|\vec{\kappa}|^2 + \eta_1 + \lambda_p \mu_2 \right) |\vec{\kappa}|^2 - |\partial_s \vec{\kappa}|^2 \right] ds. \tag{7.9}$$

Since only an $O(\varepsilon^2)$ quantity of surfactant is contained in the outer region, away from the pores and bilayers, the total mass contained in the bilayer and pores is effectively conserved, and any increase in bilayer surface area will result in a decrease of net pore length, and vice versa. Moreover the overall evolution is sensitive not only to the particular geometric configuration, that is the curvatures of Γ_p and Γ_b, but also the well-shape, through λ_b and λ_p, and the parameter η_1. The mass constraint (7.7) determines the evolution of $\mu_2(t_2)$ through the relations (7.8), and (7.9); which yield a closed, coupled system for the curvature driven flows (1.9) and (1.11). While the overall system is nontrivial to resolve in a general framework, the interaction laws of geometrically simple structures can be explicitly determined.

7.1. Competition among spherical bilayers and circular pores. We derive the interaction between spatially well-separated collections of spherically symmetric bilayers, and closed, circular pores. Indeed, at time t we suppose there are $N_b(t) \in \mathbb{N}_+$ spherical bilayer structures with radii $R_i(t)$ for $i = 1, \ldots, N_b(t)$, and $N_p(t) \in \mathbb{N}_+$ closed, circular pores of radii $r_i(t)$ for $i = 1, \ldots, N_p$, see Figure 7. To be consistent with a total surfactant phase which is $O(\varepsilon)$, we assume that each radii is $O(1)$, and $N_b = O(1)$ while $N_p = O(\varepsilon^{-1})$. Since the curvatures of the bilayers and pores are independent of position along these interfaces, the surface derivative terms in (7.8) and (7.9) are zero. In addition, in (7.8) the higher-order curvature term $K - \frac{1}{2}H^2$ is zero for a sphere in $\mathbb{R}^3$. Since the ith spherical bilayer has center-line surface area $4\pi R_i^2$, while the ith closed pore has center-line length $2\pi r_i$, we may apply (7.8) and (7.9) individually to each distinct structure, rewriting the equations as a coupled system of ordinary differential equations for the evolution of the radii,

$$\dot{R}_i = \frac{2\sigma_b}{m_b} \left(\frac{\eta_1 + \eta_2}{2} + \lambda_b \mu_2 \right) \frac{1}{R_i}, \quad i = 1, \ldots, N_b, \tag{7.10}$$

$$\dot{r}_j = \frac{\sigma_p}{m_p} \left(\frac{1}{4r_j^2} + \eta_1 + \lambda_p \mu_2 \right) \frac{1}{r_j}, \quad j = 1, \ldots, N_p. \tag{7.11}$$

The coupling is through the common, background value, $\mu_2 = \mu_2(t_2)$, of the chemical potential. Its value is determined through the conservation of mass relation, (7.7), which balances the volumes of surfactant phase in each family of structures. Simpli-

27

fying this relation, we determine

$$\mu_2(\vec{r}) = -\frac{\left(4N_b\sigma_b + \varepsilon\sigma_p \sum_{j=1}^{N_p} r_j^{-1}\right)\eta_1 + 4N_b\sigma_b\eta_2 + \frac{1}{4}\varepsilon\sigma_p \sum_{j=1}^{N_p} r_j^{-3}}{8N_b\sigma_b\lambda_b + \varepsilon\sigma_p\lambda_p \sum_{j=1}^{N_p} r_j^{-1}}. \tag{7.12}$$

The mean field μ_2 depends upon the particular values of the circular pore radii, $\vec{r} := (r_1, \cdots, r_{N_p})^t$ however it is independent of the bilayer radii, $\vec{R} := (R_1, \cdots, R_{N_b})^t$, depending only upon their total number, N_b. So long as N_b is constant the system is upper-triangular, with the pore evolution forming a closed system, while the bilayer evolution depends upon the evolution of the pores.

The equilibria form an over-constrained system, with $N_p + 1$ equations for the N_p pore radii, $\vec{r}$. From the form of (7.11) and (7.12), the pore radii take a common equilibria value

$$r_{\text{eq}} := \sqrt{\frac{\lambda_b}{2\left((\lambda_p - 2\lambda_b)\eta_1 + \lambda_p\eta_2\right)}}, \tag{7.13}$$

and evaluating the chemical potential at $\vec{r}_{\text{eq}} := (r_{\text{eq}}, \cdots, r_{\text{eq}})^T$ one obtains

$$\mu_2(\vec{r}_{\text{eq}}) = -\frac{\eta_1 + \eta_2}{2\lambda_b}, \tag{7.14}$$

which is precisely the equilibrium value for the bilayer radii. Thus, so long as the bifurcation parameter ν, defined in (1.13) is positive, then there exist equilibria consisting of N_p circular pores with common radius r_{eq} coexisting with N_b spherical bilayers of arbitrary radii, $\vec{R} \in \mathbb{R}_+^{N_b}$.

While the full dynamics of (7.10)-(7.12) are non-trivial, several important properties of the system can be readily extracted. In particular, $\mu_2 < 0$, and the spherical bilayers either all grow, if $\mu_2 > -(\eta_1+\eta_2)/(2\lambda_b)$, or all shrink, if $\mu_2 < -(\eta_1+\eta_2)/(2\lambda_b)$. Moreover, when $\nu < 0$, not only do the circular pores and spherical bilayers fail to coexist, but the spherical pores must shrink until they reach an $O(\varepsilon)$ radius. Indeed, substituting (7.12) into (7.10) and simplifying we obtain the form

$$\dot{R}_i = \frac{1}{R_i}\frac{\varepsilon\sigma_b\sigma_p}{m_b}\frac{\nu \sum_{j=1}^{N_p} r_j^{-1} - \frac{1}{2}\lambda_b \sum_{j=1}^{N_p} r_j^{-3}}{8N_b\sigma_b\lambda_b + \varepsilon\sigma_p\lambda_p \sum_{j=1}^{N_p} r_j^{-1}}, \tag{7.15}$$

which confirms that $\dot{R}_i < 0$ when $\nu < 0$. Since the radii $\vec{r}$ of the circular pores are bounded above by mass constraints, the spherical bilayers must shrink with a uniform rate, reaching an $O(\varepsilon)$ radius in an $O(1)$ time on the t_2 time-scale. At this point the interface underlying the spherical bilayer is not far from self-intersection and the analysis leading to (7.10) is no-longer valid. We conjecture that such a sufficiently small spherical bilayer will extinguish, at which instant N_b decreases by one. Although it is also plausible that a small radius bilayer may form break up into a family of micelles or form a closed-loop pore or other solution of (1.2).

On the other hand, for $\nu > 0$, the equilibrium configurations composed of N_b spherical bilayers coexisting with N_p circular pores of common radius r_{eq}, form an

asymptotically stable family. Indeed, since $\dot{R}_i$ is small near the equilibria we may assume that N_b is constant; the nonlinear asymptotic stability of the family then follows from the linear stability of $\vec{r} = \vec{r}_c$ within the closed evolution for the circular pore radii. We write this system in the form

$$\frac{d\vec{r}}{dt} = F(\vec{r}; N_b), \tag{7.16}$$

where F depends upon $\mu_2 = \mu_2(\vec{r}; N_b)$. We must determine the eigenvalues of the $N_p \times N_p$ matrix $\nabla_{\vec{r}} F(\vec{r}_c)$. We introduce the quantity $\tilde{\mu}_2(r) := \mu_2(r, \cdots, r)$, which satisfies

$$\tilde{\mu}_2 = -\frac{4\sigma_b N_b(\eta_1 + \eta_2) + \varepsilon \sigma_p N_p(\eta_1 r^{-1} + \frac{1}{4} r^{-3})}{8\sigma_b N_b \lambda_b + \varepsilon \sigma_p N_p \lambda_p r^{-1}}. \tag{7.17}$$

Taking the gradient of (7.11) and using the relation (7.14), we calculate that

$$\nabla_{\vec{r}} F(\vec{r}_{\text{eq}}) = \frac{\sigma_p}{m_p} \left(-\frac{1}{2r_{\text{eq}}^4} \mathbf{I} + \frac{\lambda_p \tilde{\mu}_2'(r_{\text{eq}})}{r_{\text{eq}}} \mathbf{O} \right),$$

where $\mathbf{O}$ denotes the $N_p \times N_p$ matrix all of whose entries are one and $\mathbf{I}$ denotes the $N_p \times N_p$ identity matrix.

The matrix $\nabla_{\vec{r}} F(\vec{r}_c)$ has an $N_p - 1$ dimensional eigenspace, given by $\ker(\mathbf{O})$, associated to the eigenvalue $\lambda_0 = -\sigma_p/(2m_p r_{\text{eq}}^4) < 0$. This eigenvalue and eigenspace establish the stability to perturbations which break the equality of the circular pore radii. The remaining eigenspace is spanned by the vector $(1, \cdots, 1)^t$ and has eigenvalue

$$\lambda_1 = \frac{\sigma_p}{m_p} \left(-\frac{1}{2r_c^4} + \frac{N_p \lambda_p \tilde{\mu}_2'(r_{\text{eq}})}{r_{\text{eq}}} \right),$$

$$= -\frac{\sigma_p}{m_p r_{\text{eq}}^4} \left(\frac{1}{2} + \frac{\varepsilon \sigma_p N_p^2 \lambda_p^2}{4(8\sigma_b N_b \lambda_b + \varepsilon \sigma_p N_p \lambda_p r_{\text{eq}}^{-1})} \right).$$

Since $\lambda_1 < 0$ this establishes the linear, and hence nonlinear asymptotic stability of the mixed equilibria, and confirms the final statement of Theorem 1.1.

REMARK 7.1. *In the absence of bilayers, when $N_b = 0$, then η_1 and η_2 drop out of the pore evolution equation, which reduces to*

$$\dot{r}_j = \frac{\pi \sigma_p}{2m_p} \left(\frac{1}{r_j^2} - \frac{\sum_{j=1}^{N_p} r_j^{-3}}{\sum_{j=1}^{N_p} r_j^{-1}} \right). \tag{7.18}$$

Any common value of the circular pore radii, $\vec{r} = (r, \cdots, r)^t$, is a stable equilibria. However adding a single spherical bilayer, in the $\nu > 0$ regime, will drive the pores to their equilibrium radius, r_{eq}, assuming the bilayer persists.

REFERENCES

[1] I. Budin and J. Szostak, *Physical effects underlying the transition from primitive to modern cell membranes*, PNAS, **108** (2011), pp. 5249-5254.

[2] J.W. Cahn and J.E. Hilliard, 1958, *Free energy of a nonuniform system I. Interfacial energy*, J. Chem. Phys., **28** (1958), pp. 258-267.

[3] A. Calini and T. Ivey, *Stability of small-amplitude torus knot solutions of the localized induction approximation*, J. Phys. A: Math. Theor. **44** (2011), 335204.

[4] F. Campelo and A. Hernández-Machado, *Model of curvature-driven pearling instability in membranes*, Physical Review Letters, **99** (2007), 088101.

[5] P. Canham, *Minimum energy of bending as a possible explanation of biconcave shape of human red blood cell*, J. Theor. Biol., **26** (1970), pp. 61-81.

[6] S. Cox and P. Matthews, *Exponential time differencing for stiff systems* Journal of Computational Physics, **176** (2002), pp. 430-455.

[7] S. Dai and Q. Du, *Motion of interfaces governed by the Cahn-Hilliard equation with highly disparate diffusion mobility*, SIAM J. Appl. Math., **72** No.6 (2012), pp. 1818-1841.

[8] S. Dai and K. Promislow, *Geometric evolution of bilayers under the functionalized Cahn-Hilliard equation*, Proc. Royal Soc. A **469** (2013), 20120505.

[9] A. Doelman, G. Hayrapetyan, K. Promislow, B. Wetton, *Meander and Pearling of Single-Curvature Bilayer interfaces*, submitted, (2013).

[10] A. Christlieb, A. Doelman, G. Hayrapetyan, J. Jones, K. Promislow, *The pearling instability in generic bilayer interfaces: weak functionalization*, preprint.

[11] Q. Du, C. Liu, and X. Wang, *Simulating the deformation of vesicle membranes under elastic bending energy in three dimensions*, J. Comp. Physics, **212** (2006), pp. 757-777.

[12] F. Lin and X. Yang , *Geometric Measure Theory – an introduction*, Advanced Mathematics, vol. 1, International Press, Boston, 2002.

[13] N. Gavish, G. Hayrapetyan, K. Promislow and L. Yang, *Curvature driven flow of bilayer interfaces*, Physica D, **240** (2011), pp. 675–693.

[14] N. Gavish, J. Jones, Z. Xu, A. Christlieb and K. Promislow, *Variational Models of Network Formation and Ion Transport: Applications to Perfluorosulfonate Ionomer Membranes*, Polymers, **4** (2012), pp. 630-655.

[15] G. Gompper and M. Schick, *Correlation between Structural and Interfacial Properties of Amphiphilic Systems*, *Phys. Rev. Lett.* **65** (1990), pp. 1116-1119.

[16] G.M. Grason and C.D. Santangelo, *Undulated cylinders of charged diblock copolymers*, European Physics Journal E, **20**(2006), pp. 335-346.

[17] G. Hayrapetyan and K. Promislow, *Spectra of Functionalized Operators*, submitted.

[18] W. Helfrich, *Elastic properties of lipid bilayers - theory and possible experiments*, Zeitshcrift fur naturforschung C, **28** (1973), pp. 693-703.

[19] W. Hsu and T. Gierke, *Ion transport and clustering in Nafion perfluorinated membranes*, Journal of Membrane Science, **13** (1983), pp. 307-326.

[20] S. Jain and F. Bates, *On the origins of morphological complexity in block copolymer surfactants*, Science, **300** (2003), pp. 460-464.

[21] S. Jain and F. Bates, *Consequences of nonergodicity in aqueous binary PEO-PB micellar dispersions*, Macromolecules, **37** (2004), pp. 1511-1523.

[22] C. Knox and G. Voth, *Probing Selected Morphological Models of Hydrated Nafion Using Large-Scale Molecular Dynamics Simulations*, The Journal of Physical Chemistry B, 144 (2010), 3205-3218.

[23] P. Loreti and R. March, *Propagation of fronts in a nonlinear fourth order equation*, Euro. Jnl. of Applied Mathematics **11** (2000), pp. 203-213.

[24] J. Lowengrub, A. Ratz and A. Voigt, *Phase-field modeling of the dynamics of multicomponent vesicles: Spinodal decomposition, coarsening, budding, and fission*, Phy. Rev. E **79** (2009), 031925-1:13.

[25] R. L. Pego , *Front migration in the nonlinear Cahn-Hilliard equation*, Proc. Royal Soc. London A **442** (1989), pp. 261-278.

[26] J. Polking, *A survey of removable singularities*, Springer-Verlag, 1988.

[27] K. Promislow and H. Zhang, *Critical points of Functionalized Lagrangians*, Discrete and Continuous Dynamical Systems, A, **33** (2013), pp. 1-16.

[28] M. Röger and R. Schätzle, *On a modified conjecture of De Giorgi*, Math. Z., **254** (2006), pp. 675-714.

[29] L. Rubatat, A. L. Rollet, G. Gebel, and O. Diat, *Evidence of elongated polymeric aggregates in Nafion*, Macromolecules, 35 (2002), pp. 4050-4055.

[30] L. Rubatat, G. Gebel and O. Diat, *Fibriallar structure of Nafion: Matching Fourier and real space studies of corresponding films and solutions*, Macromolecules, 37 (2004), pp. 7772-7783.

[31] K. Schmidt-Rohr and Q. Chen, *Parallel cylindrical water nanochannels in Nafion fuel cell membranes*, Nature Materials, 7 (2008), pp. 75-83.

[32] S. Torabi, J. Lowengrub, A. Voigt and S. Wise, *A new phase-field model for strongly aniostropic systems*, Proc. R. Soc. A, **465** (2009), pp. 1337-1359.

[33] J. Zhu, N. Ferrer, and R. Hayward, *Tuning the assembly of amphiphilic block copolymers through instabilities of solvent/water interfaces in the presence of aqueous surfactants* Soft Matter **5** (2009) pp. 2471-2478.